

Supporting Information

An easy synthetic approach to benzoporphyrins and Kröhnke type porphyrin-2-ylpyridines

Nuno M. M. Moura,^a Maria A. F. Faustino,^{a,*} Maria G. P. M. S. Neves,^{a,*} Filipe A. Almeida Paz,^b Artur M. S. Silva,^a Augusto C. Tomé,^a José A. S. Cavaleiro^a

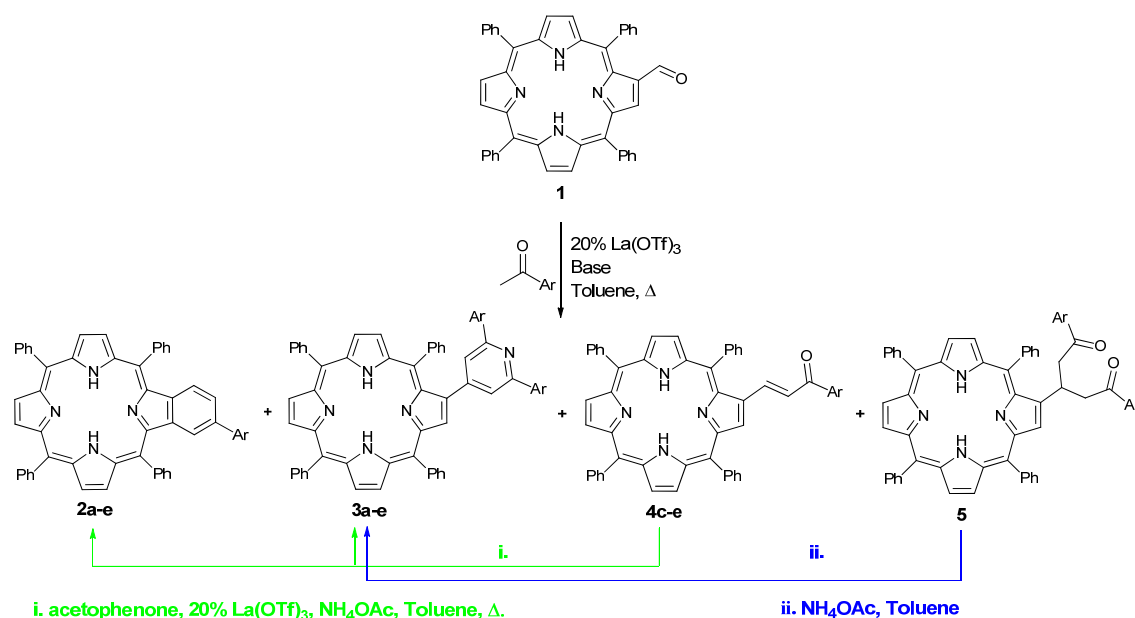
[†] Department of Chemistry and QOPNA, University of Aveiro, 3810-193 Aveiro, Portugal

[‡] Department of Chemistry and CICECO, University of Aveiro, 3810-193 Aveiro, Portugal

E-mail: faustino@ua.pt, gneves@ua.pt

Table of Contents

I - General remarks.....	S2
II - Probable mechanism of benzoporphyrin derivatives formation.....	S3
III - Experimental procedures and characterizations.....	S4
IV - ¹H and ¹³C NMR spectra.....	S11
V - X-Ray data.....	S29
References.....	S40



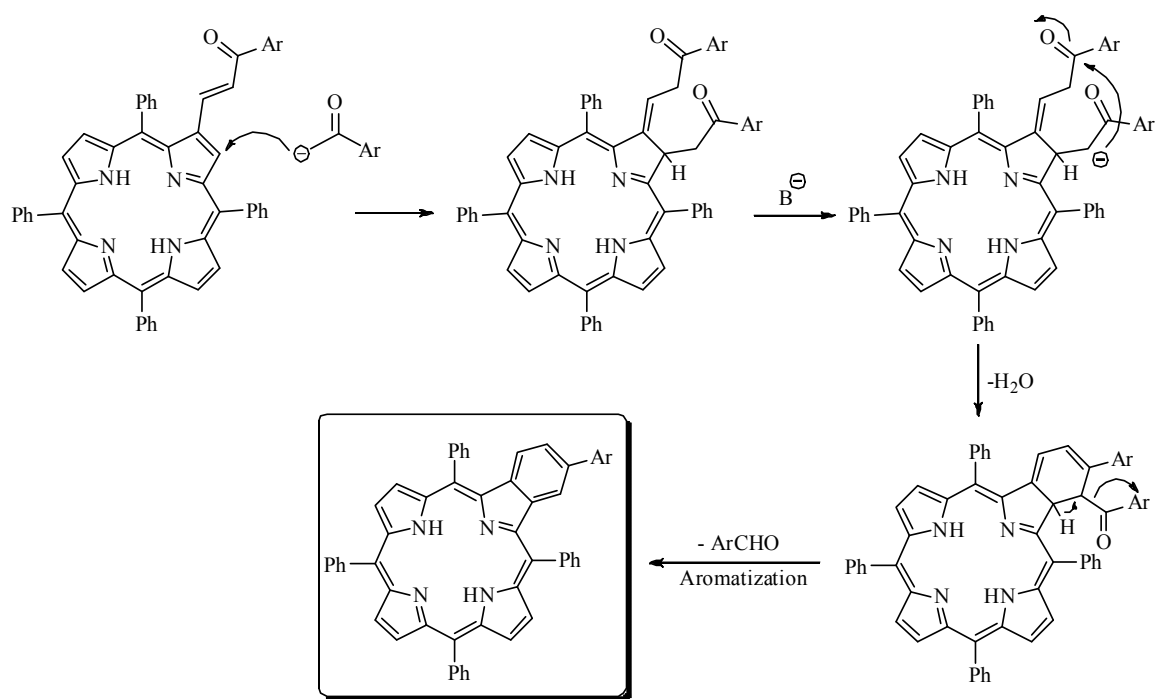
I - General remarks

¹H and ¹³C solution NMR spectra were recorded on Bruker Avance 300 (300.13 and 75.47 MHz, respectively) and 500 (500.13 and 125.76 MHz, respectively) spectrometers. CDCl₃ was used as solvent and tetramethylsilane (TMS) as internal reference; the chemical shifts are expressed in δ (ppm) and the coupling constants (*J*) in Hertz (Hz).

Unequivocal ¹H assignments were made using 2D COSY (¹H/¹H), while ¹³C assignments were made on the basis of 2D HSQC (¹H/¹³C) and HMBC (delay for long-range *J* C/H couplings were optimized for 7 Hz) experiments. Mass spectra were recorded using MALDI TOF/TOF 4800 Analyzer, Applied Biosystems MDS Sciex, with CHCl₃ as solvent and without matrix. Mass spectra HRMS were recorded on APEXQe FT-ICR (Bruker Daltonics, Billerica, MA) mass spectrometer using CHCl₃ as solvent; in *m/z* (rel. %). The UV-Vis spectra were recorded on an UV-2501 PC Shimatzu spectrophotometer using CHCl₃ as solvent. Preparative thin-layer chromatography was carried out on 20×20 cm glass plates coated with silica gel (0.5 mm thick). Column chromatography was carried out using silica gel (Merck, 35-70 mesh). Analytical TLC was carried out on precoated sheets with silica gel (Merck 60, 0.2 mm thick).

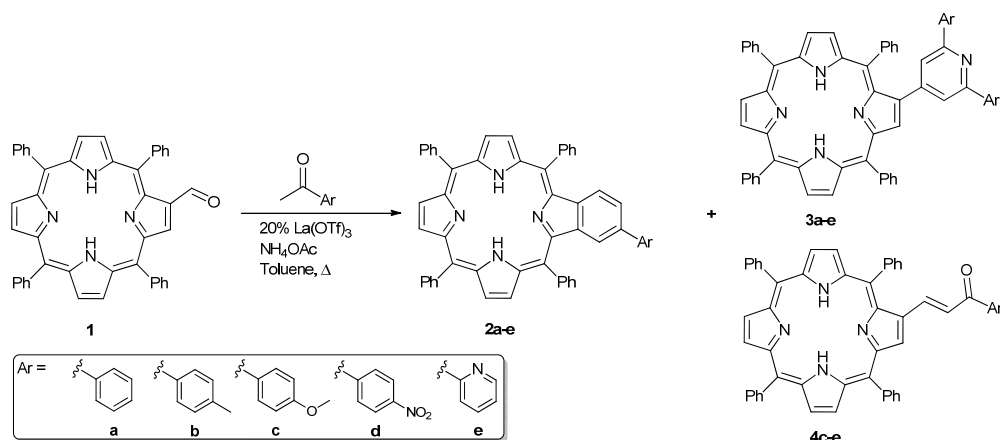
All the chemicals were used as supplied. Solvents were purified or dried according to the literature procedures.¹ The 2-formyl-5,10,15,20-tetraphenylporphyrin **1** was prepared from 5,10,15,20-tetraphenylporphyrinate copper(II), *N,N'*-dimethylformamide (DMF) and phosphorus oxychloride (POCl₃), according to literature procedure.²

II – Probable mechanism of benzoporphyrin derivatives formation



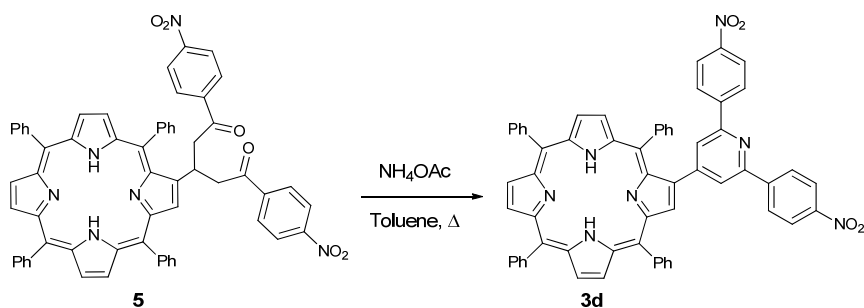
III - Experimental procedures and characterisations

1 - General procedure using ammonium acetate as base.



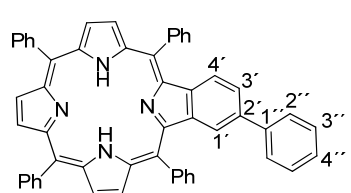
To a solution of the appropriate aryl methyl ketone (3.0 equiv.) in dry toluene (1 mL) was added ammonium acetate (4.0 equiv.) and the mixture was stirred for 30 min. at room temperature. After this time 2-formyl-5,10,15,20-tetraphenylporphyrin **1** and $\text{La}(\text{OTf})_3$ (20 mol%) were added to the mixture and it was heated at reflux for 24 h. After cooling, the reaction mixture was washed with water and extracted with chloroform. The organic phase was dried (Na_2SO_4) and the solvent was evaporated under reduced pressure. The crude mixture was submitted to column chromatography (silica gel) using toluene/light petroleum (1:1) and toluene as eluent. The fractions obtained were full characterized by NMR, mass and UV-Vis techniques.

2 - Experimental procedure for the preparation of compound **3d** from **5**.



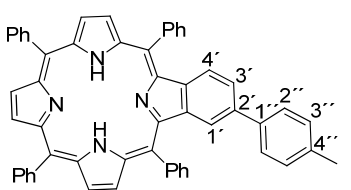
A solution of compound **5** (4.0 mg, 4.2 μ mol) and NH₄OAc (1.0 mg, 12.6 μ mol, 3.0 equiv) in dry toluene (1 mL) was stirred at refluxing temperature for 24 hours. After this time no starting material **5** was detected by TLC. After cooling, the reaction mixture was washed with water and extracted with chloroform. The organic phase was dried (Na₂SO₄) and evaporated under reduced pressure. The mixture was submitted to column chromatography (silica gel) using toluene/ light petroleum (1:1) and toluene as the eluents. Two fractions were isolated: one corresponding to porphyrin-pyridine derivative **3d** (3.2 mg, 82% yield) and the other corresponding to unchanged compound **5** (8% recovered).

Compound 2a



¹H NMR (300 MHz, CDCl₃): δ 8.93 (1H, d, *J* = 5.1 Hz, H- β), 8.91 (1H, d, *J* = 5.1 Hz, H- β), 8.85 (1H, d, *J* = 4.8 Hz, H- β), 8.83 (1H, d, *J* = 4.8 Hz, H- β), 8.72 (2H, AB, *J* = 4.8 Hz, H- β), 8.24-8.20 (8H, m, H-*o*-Ph), 7.92-7.73 (16H, m, H-*m,p*-Ph, H-1', H-3', H-2'', 6'', H-3'', 5'' and H-4''), 7.42-7.40 (3H, m, H-*m,p*-Ph), 7.26 (1H, d, H-4', *J* = 8.5 Hz), -2.65 (2H, s, N-H) ppm. ¹³C NMR (125 MHz, CDCl₃): δ 154.3 (C- α), 143.1, 142.3, 142.0, 141.9, 139.1 (C- α), 138.6 (C- α), 138.0 (C- α), 134.5 (C-*o*-Ph), 134.1 (C- β), 133.9, 133.8, 133.6, 133.4, 132.6, 132.3 (C-4'), 129.0, 128.9, 128.6, 128.3, 128.2, 127.9, 127.80, 127.75, 127.6, 127.4, 127.05, 126.98, 126.8, 126.7 (C-*o,m*-Ph, C-1', C-2'', 6'', C-3'', 5'' and C-4''), 125.3, 121.1 (C-*meso*), 121.0 (C-*meso*), 117.8 (C-*meso*), 117.5 (C-*meso*), 116.7 (C-3') ppm. UV-Vis (CHCl₃) λ_{max} (log ϵ) 427.0 (5.27), 519.0 (3.99), 593.5 (3.53) nm. MS (MALDI): 741.3 [M+H]⁺. HRMS-ESI *m/z* C₅₄H₃₇N₄ for [M+H]⁺ calcd 741.3019, found 741.3003.

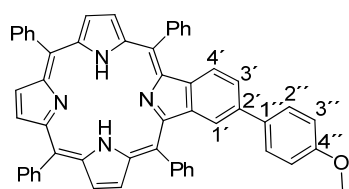
Compound 2b



¹H NMR (300 MHz, CDCl₃): 8.91 (1H, d, *J* = 5.0 Hz, H- β), 8.89 (1H, d, *J* = 5.0 Hz, H- β), 8.83 (1H, d, *J* = 5.0 Hz, H- β), 8.81 (1H, d, *J* = 5.0 Hz, H- β), 8.72 (2H, AB, *J* = 5.1 Hz, H- β), 8.24-8.19 (8H, m, H-*o*-Ph), 8.09 (1H, d, *J* = 8.2 Hz, H-3'), 7.91-7.73 (12H, m, H-*m,p*-Ph and H-1') 7.72 (1H, AB, *J* = 8.2 Hz, H-2'', 6''), 7.30 (1H, d, *J* = 8.2 Hz, H-4'), 7.21 (2H, AB, *J* = 8.2 Hz, H-3'', 5''), 2.42 (3H, s, CH₃), -2.66 (2H, s, N-H) ppm. ¹³C NMR (75 MHz, CDCl₃): δ 157.3, 154.4 (C- α),

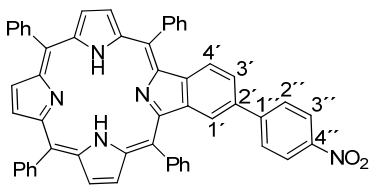
149.8 (C-2'), 143.2, 142.3, 142.0, 141.9, 138.9 (C- α), 138.8 (C- α), 137.9 (C- α) 137.0, 136.4, 134.5, 134.1, 133.9, 133.8 (C- β), 133.6, 133.2, 132.2, 129.8, 129.4, 129.3, 129.0, 128.5, 128.2 (C-1'), 127.9 (C- β), 127.8 (C- β), 127.7, 127.6 (C- β), 127.3 (C-*p*-Ph), 127.0, 126.9 (C- β), 126.8 (C-*m*-Ph), 126.7 (C-*m*-Ph), 121.1 (C-*meso*), 121.0 (C-*meso*), 117.8 (C-*meso*), 117.5 (C-*meso*), 116.4 (C-3'), 116.3 (C-3'',5''), 21.3 (CH_3) ppm. UV-Vis (CHCl_3) λ_{max} ($\log \epsilon$) 427.5 (5.28), 519.0 (4.35), 590.0 (3.88) nm. MS (MALDI): 755.2 [$\text{M}+\text{H}$]⁺. HRMS-ESI *m/z* C₅₅H₃₉N₄ for [M+H]⁺ calcd 755.3122, found 755.3104.

Compound 2c



¹H NMR (500 MHz, CDCl_3): 8.91 (1H, d, *J* = 5.1 Hz, H- β), 8.91 (1H, d, *J* = 5.1 Hz, H- β), 8.82 (1H, d, *J* = 4.9 Hz, H- β), 8.81 (1H, d, *J* = 4.9 Hz, H- β), 8.72 (2H, AB, *J* = 5.1 Hz, H- β), 8.25-8.19 (8H, m, H-*o*-Ph), 7.91-7.71 (16H, m, H-*m,p*-Ph, H-1', H-3' and H-2'',6''), 7.20 (1H, d, *J* = 8.6 Hz, H-4'), 6.93 (2H, d, *J* = 8.9 Hz, H-3'',5''), 3.91 (3H, s, OCH₃), -2.65 (2H, s, N-H) ppm. ¹³C NMR (75 MHz, CDCl_3): δ 160.5, 154.1 (C- α), 152.3 (C-2'), 143.2, 142.3, 142.0, 141.9, 134.5 (C-*o*-Ph), 134.1 (C- β), 133.9, 133.8, 133.6, 132.8, 132.3, 131.9 (C-4'), 128.8 (C-1'), 128.5 (C- β), 128.2 (C-2'',6'') 127.9 (C-*m*-Ph), 127.8(C- β), 127.7 (C-*p*-Ph), 127.5, 126.9 (C-*m*-Ph), 126.8 (C-*m*-Ph), 126.7 (C-*m*-Ph), 121.1 (C-*meso*), 121.0 (C-*meso*), 117.7 (C-*meso*), 117.4 (C-*meso*), 116.0 (C-3'), 113.6 (C-3'',5''), 55.4 (OCH₃) ppm. UV-Vis (CHCl_3) λ_{max} ($\log \epsilon$) 427.0 (5.46), 519.0 (4.32), 593.5 (3.85) nm. MS (MALDI): 770.2 [M]⁺. HRMS-ESI *m/z* C₅₅H₃₈N₄O for [M]⁺ calcd 770.2901, found 770.2901.

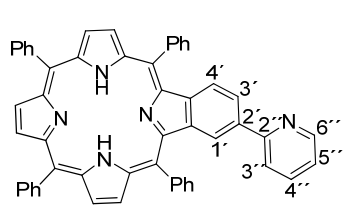
Compound 2d



¹H NMR (300 MHz, CDCl_3): δ 8.94 (1H, d, *J* = 5.1 Hz, H- β), 8.92 (1H, d, *J* = 5.1 Hz, H- β), 8.85 (1H, d, H- β , *J* = 5.0 Hz), 8.82 (1H, d, H- β , *J* = 5.0 Hz), 8.73 (2H, AB, *J* = 4.6 Hz, H- β), 8.26-8.19 (10H, m, H-*o*-Ph and H-3'',5''), 7.96-7.73 (16H, m, H-*m,p*-Ph, H-2'',6'', H-1' and H-3'), 7.29 (1H, d, *J* = 8.5 Hz, H-4'), -2.67 (2H, s, N-H) ppm. ¹³C NMR (75 MHz, CDCl_3): δ 159.9, 154.9 (C- α), 151.4 (C-2'), 147.9 (C-4''), 147.6 (C- α), 146.1 (C- α), 145.2 (C-1''), 143.1, 142.1, 141.8, 141.7, 140.2 (C- α), 138.8 (C- α), 138.1 (C- α), 134.5 (C-*o*-Ph), 134.2 (C- β), 134.1, 133.5, 132.6 (C-4'), 128.7 (C-1'), 128.4 (C- β), 128.2 (C- β), 128.1 (C-3'',5''), 128.0 (C-

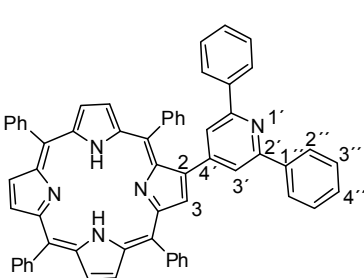
m-Ph), 127.9 (*C-m*-Ph), 127.8 (*C*- β), 127.2 (*C-p*-Ph), 127.0, 126.80 (*C-m*-Ph), 126.77 (*C-m*-Ph), 123.6 (*C-2'',6''*), 121.34 (*C-meso*), 121.30 (*C-meso*), 117.8 (*C-meso*), 117.7 (*C-meso*), 117.4 (*C-3'*) ppm. UV-Vis (CHCl_3) λ_{\max} ($\log \epsilon$) 430.0 (5.24), 521.0 (4.22), 595.0 (3.76) nm. MS (MALDI): 786.2 [$\text{M}+\text{H}]^+$. HRMS-ESI *m/z* for $\text{C}_{54}\text{H}_{36}\text{N}_5\text{O}_2$ [$\text{M}+\text{H}]^+$ calcd 786.2816, found 786.2799.

Compound 2e



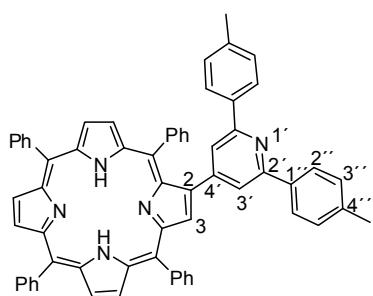
^1H NMR (500 MHz, CDCl_3): δ 8.92 (1H, d, *J* = 5.0 Hz, H- β), 8.90 (1H, d, *J* = 5.0 Hz, H- β), 8.87 (1H, d, *J* = 4.9 Hz, H- β), 8.82 (1H, d, *J* = 4.9 Hz, H- β), 8.73 (2H, AB, *J* = 4.9, H- β), 8.65-8.64 (1H, ddd, *J* = 1.6 and 4.7 Hz, H-6''), 8.48 (1H, d, *J* = 8.4 Hz, H-3''), 8.26-8.20 (8H, m, H-*o*-Ph), 7.91-7.72 (15H, m, H-*m,p*-Ph, H-1', H-3' and H-4''), 7.29-7.26 (2H, m, H-4' and H-5''), -2.65 (2H, s, N-H) ppm. ^{13}C NMR (125 MHz, CDCl_3): δ 159.5, 156.7, 153.7, 148.8, 143.3, 142.1, 141.98, 141.87, 140.2, 138.9, 137.9, 136.3, 134.8, 134.5, 134.2, 133.9, 133.6, 132.6, 129.0, 128.6, 128.22, 128.17, 127.9, 127.85-127.71 (*C*- β), 127.80, 127.75, 126.94, 126.92, 126.8, 126.7, 125.3, 123.5, 122.2, 121.2, 117.84, 117.75, 117.6 ppm. UV-Vis (CHCl_3) λ_{\max} ($\log \epsilon$) 427.5 (5.51), 519.5 (4.30), 594.0 (3.83) nm. MS (MALDI): 742.2 [$\text{M}+\text{H}]^+$. HRMS-ESI *m/z* $\text{C}_{53}\text{H}_{36}\text{N}_5$ for [$\text{M}+\text{H}]^+$ calcd 742.2918, found 742.2906.

Compound 3a



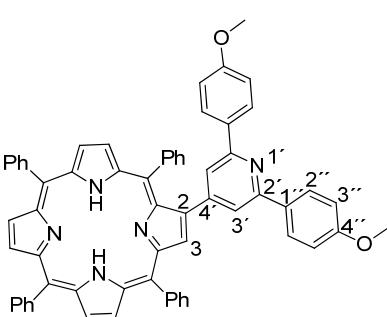
^1H NMR (300 MHz, CDCl_3): δ 8.87-8.79 (7H, m, H- β), 8.26-8.20 (6H, m, H-*o*-Ph), 8.13-8.09 (4H, m, H-2'',6''), 8.00-7.97 (2H, m, H-*o*-Ph), 7.77-7.71 (9H, m, H-*m,p*-Ph), 7.63 (2H, s, H-3''), 7.52-7.42 (6H, m, H-3'',5'' and H-4''), 7.14-7.11 (3H, m, H-*m,p*-Ph), -2.61 (2H, s, N-H) ppm. ^{13}C NMR (75 MHz, CDCl_3): δ 155.6, 148.6, 142.2, 142.1, 141.8, 140.3, 139.6, 135.6, 134.6, 134.5, 132.3-130.2 (*C*- β), 128.7, 128.6, 128.0, 127.9, 127.8, 127.1, 126.8, 126.7, 126.1, 121.0, 120.6, 120.5, 120.2 ppm. UV-Vis (CHCl_3) λ_{\max} ($\log \epsilon$) 422.5 (5.33), 518.5 (4.01), 554.0 (3.59), 593.5 (3.50), 650.0 (3.33) nm. MS (MALDI): 843.3 [$\text{M}]^+$. HRMS-ESI *m/z* $\text{C}_{61}\text{H}_{42}\text{N}_5$ for [$\text{M}+\text{H}]^+$ calcd 844.3435, found 844.3411.

Compound 3b



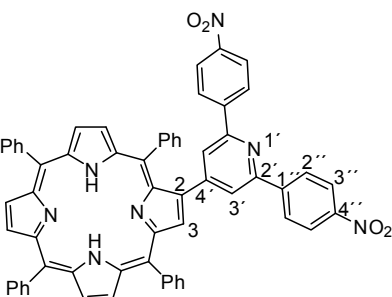
¹H NMR (300 MHz, CDCl₃): δ 8.87-8.79 (7H, m, H-β), 8.25-8.20 (6H, m, H- H-*o*-Ph), 8.01 (4H, AB, *J* = 8.2 Hz, H-2'',6''), 9.99-7.96 (2H, m, H-*o*-Ph), 7.78-7.71 (9H, m, H-*m,p*-Ph), 7.57 (2H, s, H-3'), 7.29 (4H, AB, *J* = 8.2 Hz, H-3'',5''), 7.14-7.12 (3H, m, H-*m,p*-Ph), 2.42 (6H, s, CH₃), -2.64 (2H, s, N-H) ppm. ¹³C NMR (75 MHz, CDCl₃): δ 155.5, 148.3, 142.2, 142.1, 141.8, 140.2, 138.6, 137.0, 135.5, 134.6, 134.5, 132.2-130.2 (C-β), 129.3, 129.0, 128.2, 128.0, 127.85, 127.77, 127.0, 126.8, 126.7, 126.1, 121.0, 120.5, 120.2, 120.0, 21.3 (CH₃) ppm. UV-Vis (CHCl₃) λ_{max} (log ε) 426.0 (4.99), 518.0 (4.29), 554.0 (3.86), 593.5 (3.76), 649.5 (3.58) nm. MS (MALDI): 872.3 [M+H]⁺. HRMS-ESI *m/z* C₆₃H₄₆N₅ for [M+H]⁺ calcd 872.3748, found 872.3736.

Compound 3c



¹H NMR (300 MHz, CDCl₃): δ 8.89-8.79 (7H, m, H-β), 8.26-8.21 (6H, m, H-*o*-Ph), 8.06 (4H, AB, *J* = 8.9 Hz, H-2'',6''), 7.99-7.96 (2H, m, H-*o*-Ph), 7.78-7.70 (9H, m, H-*m,p*-Ph), 7.51 (2H, s, H-3'), 7.16-7.12 (3H, m, H-*m*-Ph), 7.02 (4H, AB, *J* = 8.9 Hz, H-3'',5''), 3.88 (6H, s, OCH₃), -2.63 (2H, s, N-H) ppm. ¹³C NMR (75 MHz, CDCl₃): δ 160.2, 155.1, 148.2, 142.2, 142.1, 141.8, 140.3, 135.5, 134.6, 134.5, 132.5, 132.1-130.2 (C-β), 129.0, 128.3, 128.2, 128.0, 127.85, 127.78, 126.8, 126.7, 126.6, 126.1, 121.0, 120.5, 120.2, 119.3, 113.9, 55.4 (OCH₃). UV-Vis (CHCl₃) λ_{max} (log ε) 422.0 (5.38), 518.5 (4.15), 553.5 (3.75), 592.5 (3.64), 648.5 (3.45) nm. MS (MALDI): 904.3 [M+H]⁺. HRMS-ESI *m/z* C₆₃H₄₆N₅O₂ for [M+H]⁺ calcd 904.3646, found 904.3626.

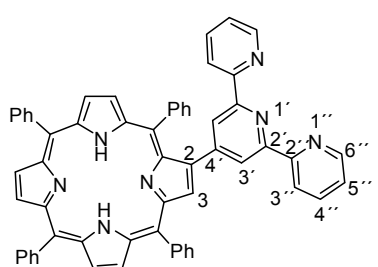
Compound 3d



¹H NMR (300 MHz, CDCl₃): δ 8.84-8.77 (7H, m, H-β), 8.38 and 8.28 (8H, AB, *J* = 8.9 Hz, H-2'',6'' and H-3'',5''), 8.33-8.20 (6H, m, H-*o*-Ph), 8.00-7.97 (2H, m, H-*o*-Ar), 7.80-7.73 (11H, m, H-3' and H-*m,p*-Ph), 7.11-7.09 (3H, m, H-*m*-Ph), -2.64 (2H, s, N-H) ppm.

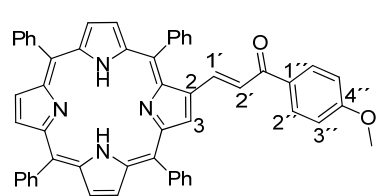
¹³C NMR (75 MHz, CDCl₃) δ 153.5, 148.2, 144.9, 142.1, 141.60, 140.58, 135.7, 134.6, 134.5, 132.4-130.2 (C-β), 129.3, 129.0, 128.2, 128.05, 127.98, 127.9, 127.8, 126.9, 126.8, 126.1, 124.0, 123.9, 122.8, 122.4, 120.8, 120.5, 120.38, 120.35. UV-Vis (CHCl₃) λ_{max} (log ε) 423.0 (5.32), 519.0 (4.05), 554.0 (3.61), 594.0 (3.52), 650.0 (3.40) nm. MS (MALDI): 934.3 [M+H]⁺. HRMS-ESI *m/z* C₆₁H₄₀N₇O₄ for [M+H]⁺ calcd 934.3136, found 934.3114.

Compound 3e



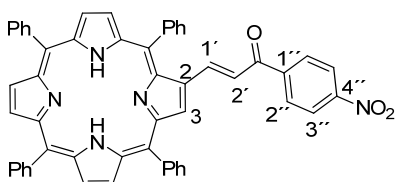
¹H NMR (500 MHz, CDCl₃): δ 8.89 (1H, s, H-3), 8.87-8.82 (4H, m, H-β), 8.77 and 8.76 (2H, AB, *J* = 4.9 Hz, H-β), 8.67-8.63 (4H, m, H-*o*-Ph and H-6''), 8.38 (2H, s, H-3''), 8.25-8.21 (6H, m, H-*o*-Ph), 7.97 (2H, d, *J* = 7.8 Hz, H-3''), 7.90 (2H, dt, *J* = 1.5 and 7.8 Hz, H-4''), 7.79-7.71 (9H, m, H-*m,p*-Ph), 7.35-7.33 (2H, ddd, *J* = 1.2, 4.7 and 7.8 Hz, H-5''), 7.01-6.98 (3H, m, H-*m*-Ph), -2.63 (2H, s, N-H) ppm. ¹³C NMR (125 MHz, CDCl₃) δ 156.4, 154.1, 149.1, 142.2, 141.9, 140.5, 136.7, 135.8, 134.6, 134.5, 131.6-129.2 (C-β), 127.8, 127.7, 127.6, 126.8, 126.70, 126.66, 125.95, 123.5, 122.7, 121.3, 121.0, 120.34, 120.28, 120.1 ppm. UV-Vis (CHCl₃) λ_{max} (log ε) 422.5 (5.43), 519.0 (4.21), 554.5 (3.76), 594.5 (3.68), 650.5 (3.47) nm. MS (MALDI): 846.3 [M+H]⁺. HRMS-ESI *m/z* C₅₉H₄₀N₇ for [M+H]⁺ calcd 846.3340, found 846.3323.

Compound 4c



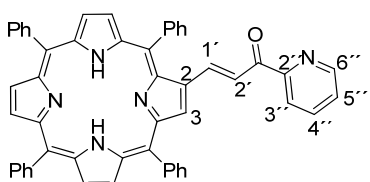
¹H NMR (300 MHz, CDCl₃): δ 9.05 (1H, s, H-3), 8.85-8.76 (6H, m, H-β), 8.25-8.18 (6H, m, H-*o*-Ph), 8.10-8.07 (2H, m, H-*o*-Ph), 7.96 (2H, AB, *J* = 8.9 Hz, H-2'',6''), 7.81-7.65 (12H, m, H-*m,p*-Ph), 7.55 and 7.47 (2H, AB, *J* = 15.3 Hz, H-1' and H-2'), 7.00 (2H, AB, *J* = 8.9 Hz, H-3''5''), 3.92 (3H, s, OCH₃), -2.59 (2H, s, N-H) ppm. ¹³C NMR (75 MHz, CDCl₃): δ 189.5 (C=O), 163.1, 142.2, 142.0, 141.7, 141.3, 140.2, 134.6, 134.5, 134.1, 131.6, 131.2, 130.9, 130.2, 129.0, 128.7, 128.2, 128.7, 127.8, 127.1, 126.80, 126.76, 126.7, 124.3, 120.5, 120.4, 120.1, 113.7 (C-3'',5''), 55.5 (OCH₃) ppm. UV-Vis (CHCl₃) λ_{max} (log ε) 433.5 (5.20), 524.5 (4.20), 567.5 (3.83), 601.5 (3.74), 659.0 (3.45) nm. MS (MALDI): 775.3 [M+H]⁺. HRMS-ESI *m/z* for C₅₄H₃₈N₄O₂ [M]⁺ calcd 774.2995, found 774.2988.

Compound 4d



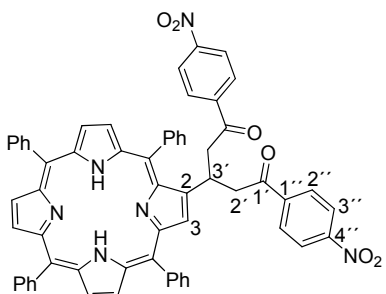
¹H NMR (300 MHz, CDCl₃): δ 9.10 (1H, s, H-3), 8.85 (2H, AB, *J* = 5.1 Hz, H-β), 8.81-8.79 (3H, m, H-β), 8.73 (1H, AB, *J* = 4.8 Hz, H-β), 8.34 (2H, d, *J* = 8.8 Hz, H-3'',5''), 8.25-8.17 (6H, m, H-*o*-Ph), 8.08-8.05 (2H, m, H-*o*-Ph), 7.96 (2H, AB, *J* = 8.8 Hz, H-2'',6''), 7.82-7.74 (9H, m, H-*m,p*-Ph), 7.57-7.55 (3H, m, H-*m*-Ph), 7.45 (2H, AB, *J* = 15.6 Hz, H-1' and H-2'), -2.57 (2H, s, N-H) ppm. ¹³C NMR (75 MHz, CDCl₃): δ 190.7 (C=O), 150.3, 149.6, 143.4, 143.3, 142.0, 141.8, 141.6, 141.5, 134.54, 134.52, 134.2, 133.1-130.0 (C-β), 129.6, 129.0, 128.6, 128.55, 128.50, 128.3, 128.2, 128.1, 127.9, 127.0, 126.84, 126.80, 126.7, 124.1, 123.6, 120.8, 120.5, 120.4, 120.1 ppm. UV-Vis (CHCl₃) λ_{max} (log ε) 434.0 (5.05), 526.5 (4.08), 570.5 (3.62), 603.0 (3.60), 663.5 (3.30) nm. MS (MALDI): 790.2 [M+H]⁺. HRMS-ESI *m/z* for C₅₃H₃₆N₅O₃ [M+H]⁺ calcd 790.2813, found 790.2798.

Compound 4e



¹H NMR (300 MHz, CDCl₃): δ 9.18 (1H, s, H-3), 8.84-8.79 (6H, m, H-β), 8.75 (1H, d, *J* = 4.7 Hz, H-6''), 8.25-8.13 (8H, m, H-*o*-Ph and H-3''), 7.89 (1H, dt, *J* = 1.6 and 7.8 Hz, H-4''), 7.79-7.69 (14H, m, H-*m,p*-Ph, H-1' and H-2'), 7.49 (1H, ddd, *J* = 1.3, 4.7 and 7.8 ,H-5''), -2.56 (2H, s, N-H) ppm. ¹³C NMR (75 MHz, CDCl₃): δ 189.4 (C=O), 154.6, 148.7, 142.1, 142.0, 141.7, 141.5, 141.3, 137.0, 134.6, 134.5, 134.3, 131.9-30.5 (C-β), 129.0, 128.7, 128.5, 127.9, 127.8, 127.2, 126.8, 126.7, 126.6, 123.1, 122.4, 120.7, 120.4, 120.3, 120.2 ppm. UV-Vis (CHCl₃) λ_{max} (log ε) 437.5 (5.05), 525.5 (4.15), 572.0 (3.83), 602.5 (3.74), 662.0 (3.44) nm. MS (MALDI): 746.2 [M+H]⁺. HRMS-ESI *m/z* for C₅₂H₃₆N₅O [M+H]⁺ calcd 746.2914, found 746.2906.

Compound 5



¹H NMR (300 MHz, CDCl₃): δ 8.84-8.81 (3H, m, H-β), 8.75-8.69 (3H, m, H-β), 8.46 (1H, d, *J* = 4.9 Hz, H-β), 8.22-8.09 (6H, m, H-*o*-Ph), 8.11 (4H, AB, *J* = 8.9 Hz, H-3'',5''), 7.96-7.93 (2H, m, H-*o*-Ph), 7.90 (4H, AB, *J* = 8.9 Hz, H-2'',6''), 7.78-7.65 (10H, m, H-*m,p*-

Ph), 7.42 (2H, t, J = 7.7 Hz, H-*m*-Ph), 4.48-4.38 (1H, m, H-3'), 3.63 (4H, dq, J = 6.8 and 17.1 Hz, H-2'), -2.80 (2H, s, N-H) ppm. ^{13}C NMR (75 MHz, CDCl_3) δ 196.9 ($\text{C}=\text{O}$), 150.1, 142.4, 142.0, 141.5, 141.1, 134.6, 134.5, 133.3, 131.8-130.5 (C- β), 129.0, 128.4, 128.2, 127.8, 127.0, 126.8, 126.65, 126.59, 125.3, 123.7, 120.6, 120.4, 119.3, 119.2, 46.1 (C-3'), 30.9 (C-2') ppm. UV-Vis (CHCl_3) λ_{max} (log ε) 421.0 (5.39), 517.5 (4.28), 551.5 (3.87), 591.5 (3.75), 647.5 (3.46) nm. MS (MALDI): 955.3 [M+H] $^+$. HRMS-ESI m/z $\text{C}_{61}\text{H}_{43}\text{N}_6\text{O}_6$ for [M+H] $^+$ calcd 955.3239, found 955.3224.

IV- ^1H and ^{13}C NMR spectra

➤ Compounds 2a-f:

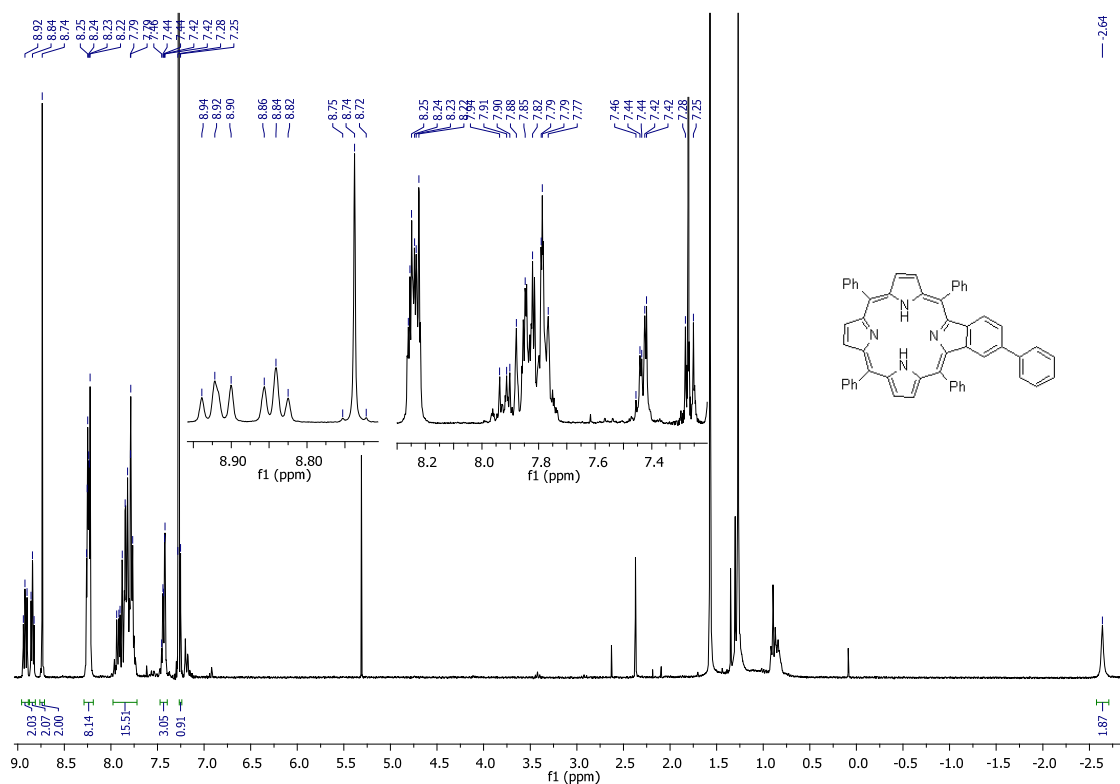
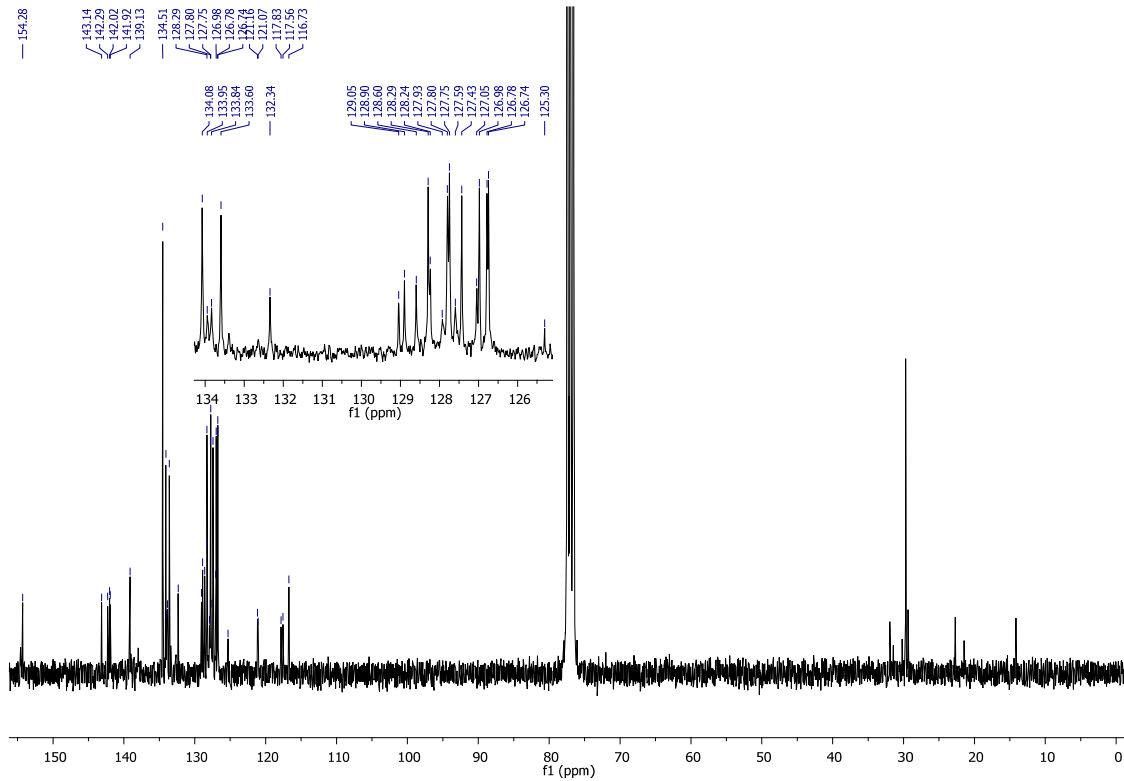


Figure S1 – ^1H NMR spectrum of compound 2a.



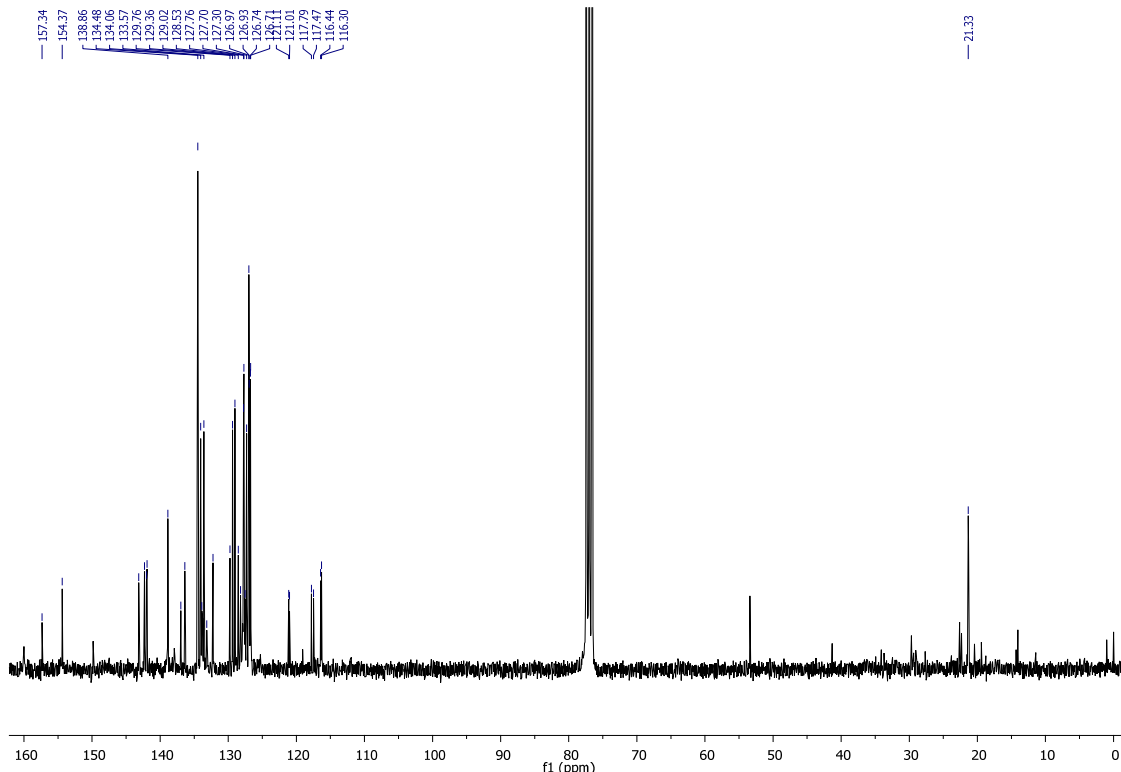


Figure S4 – ¹³C NMR spectrum of compound 2b.

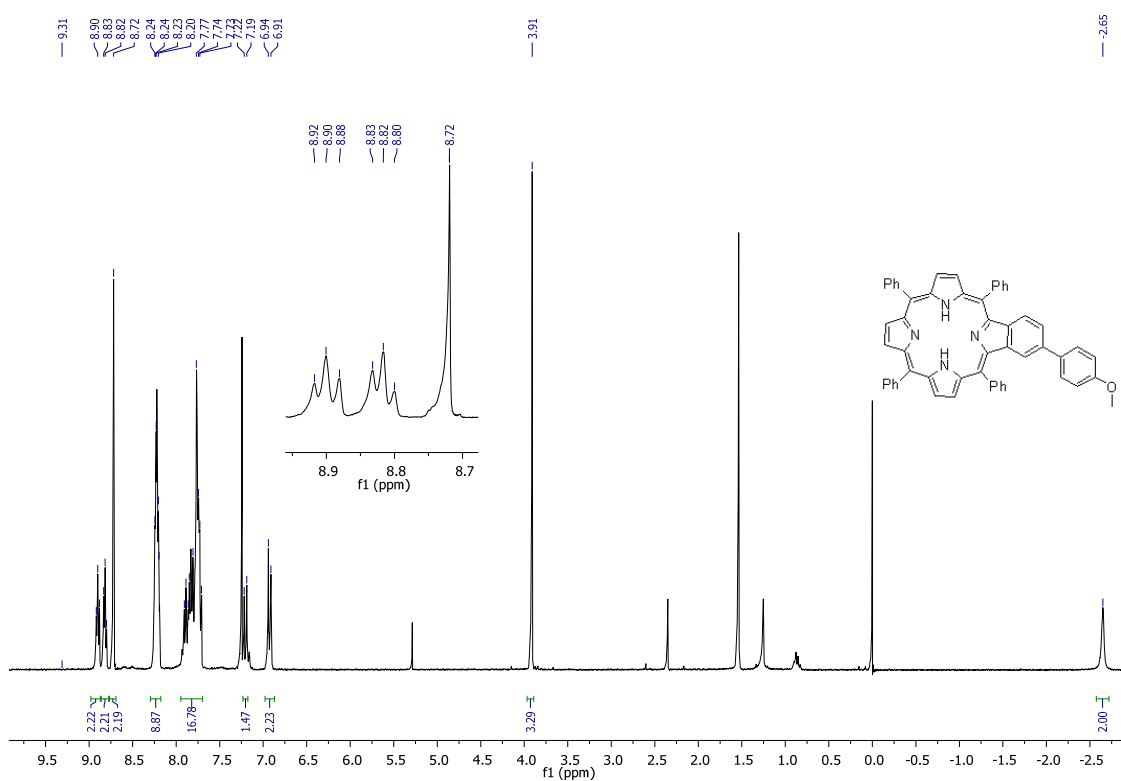


Figure S5 – ¹H NMR spectrum of compound 2c.

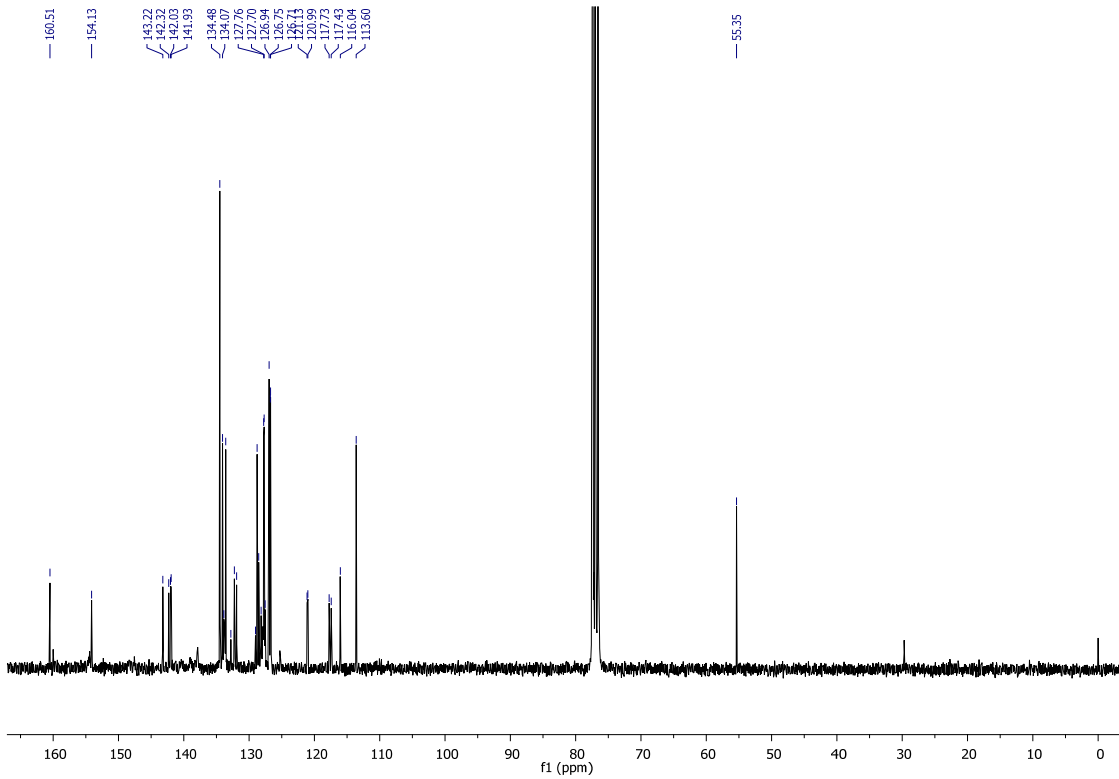


Figure S6 – ^{13}C NMR spectrum of compound 2c.

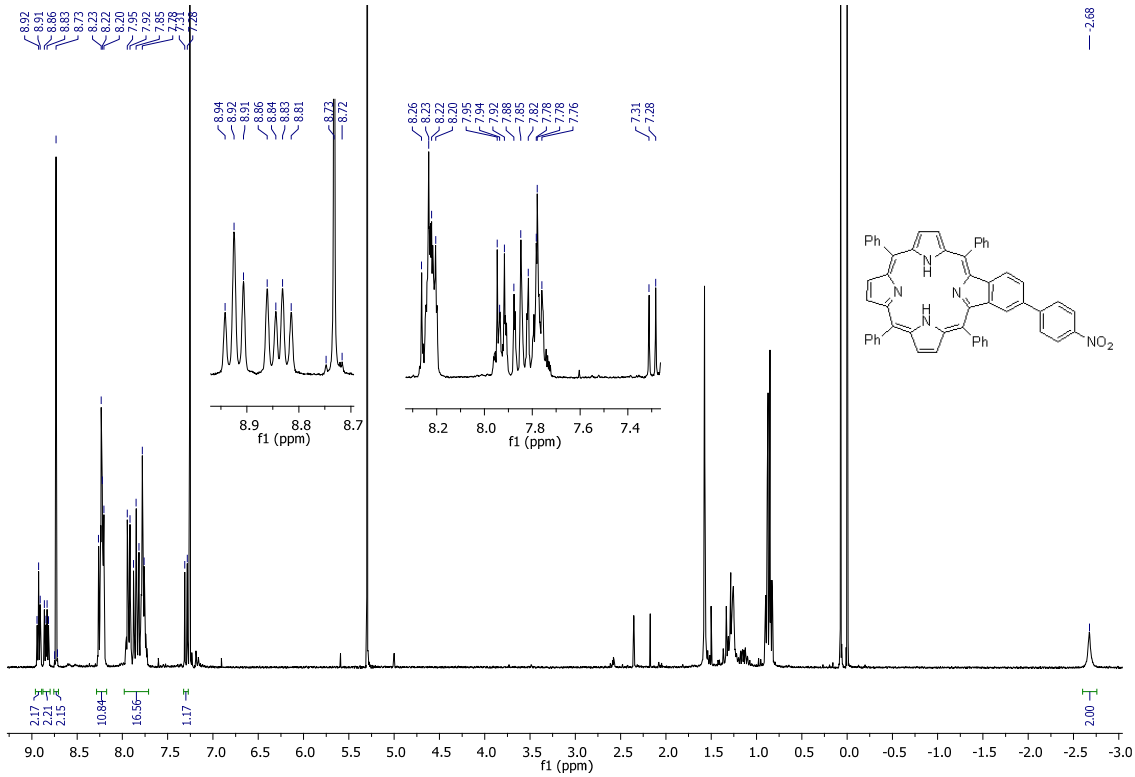


Figure S7 – ^1H NMR spectrum of compound 2d.

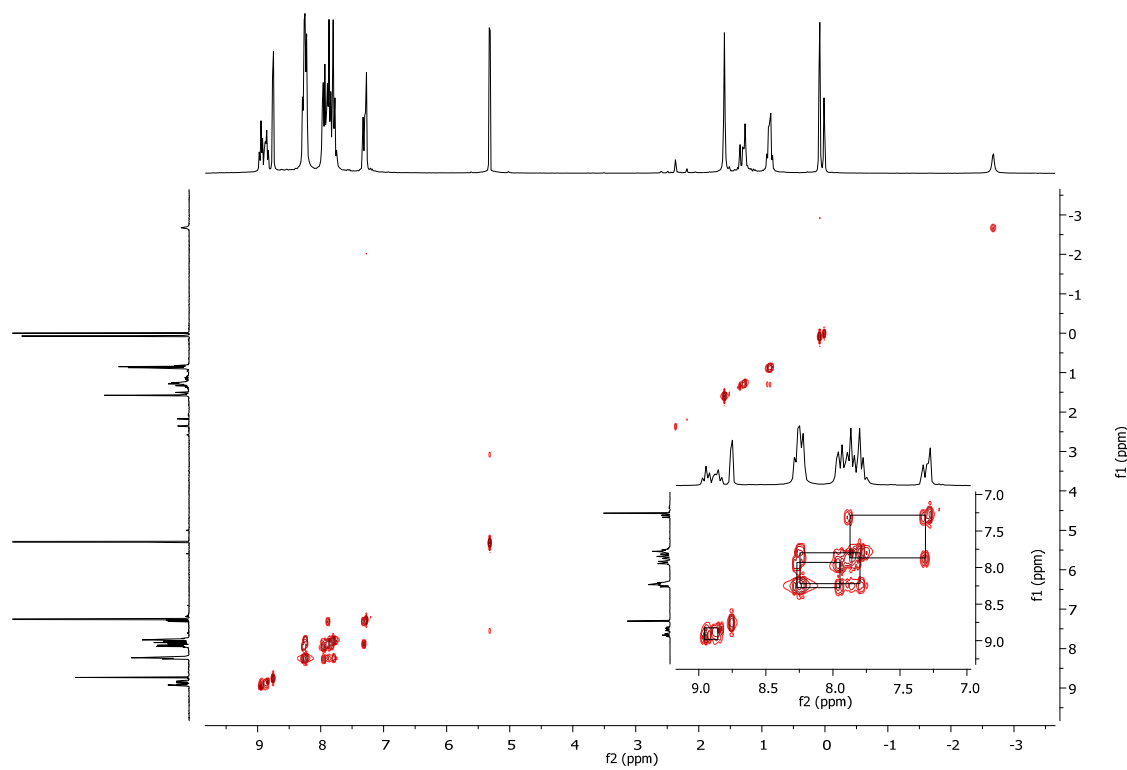


Figure S8 –COSY spectrum of compound 2d.

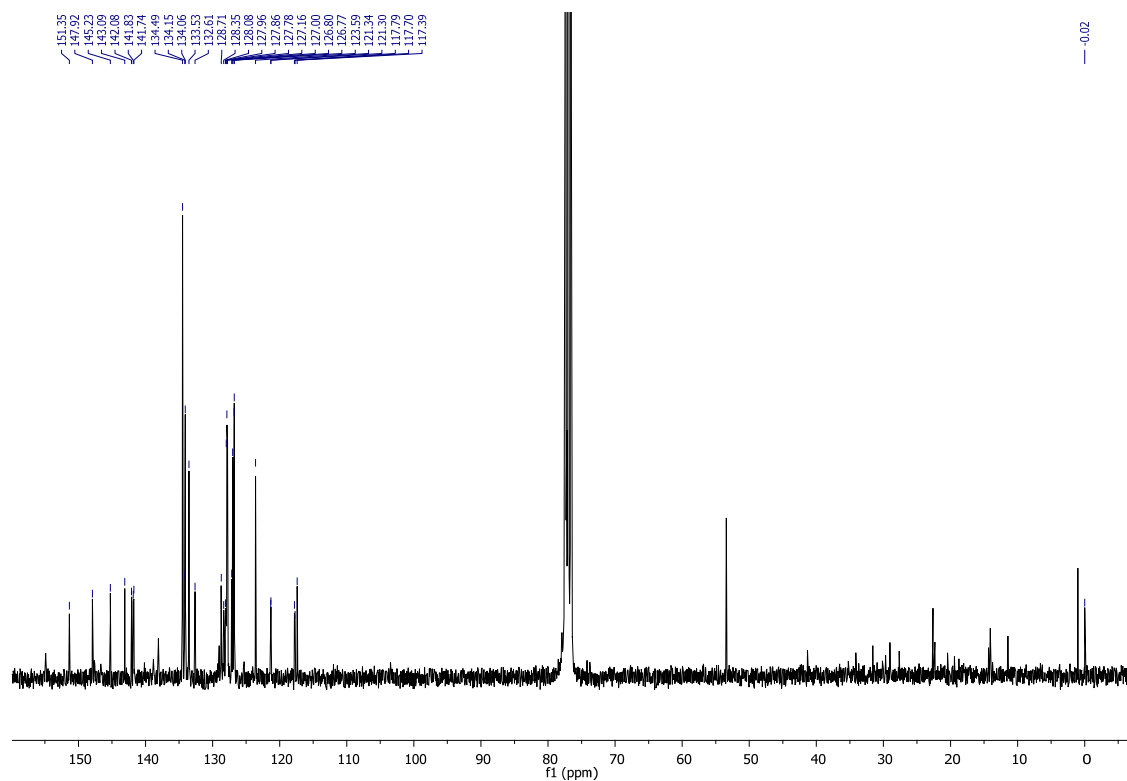


Figure S9 – ^{13}C NMR spectrum of compound 2d.

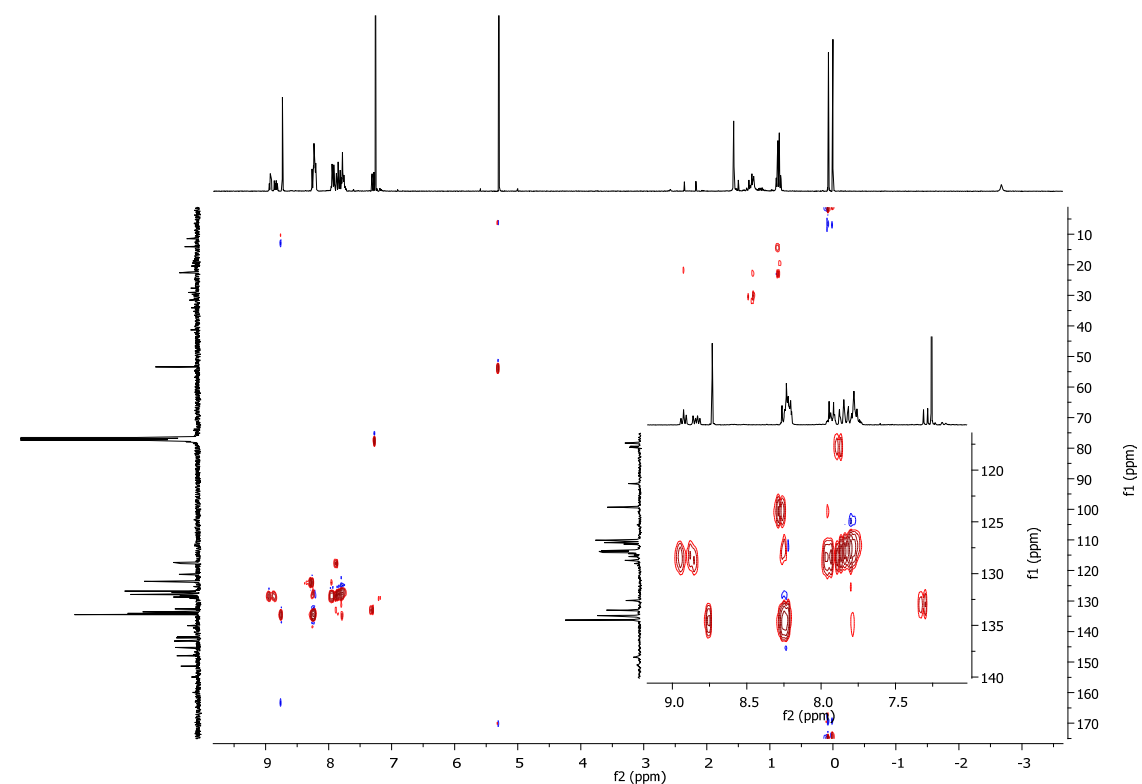


Figure S10 – HSQC spectrum of compound 2d.

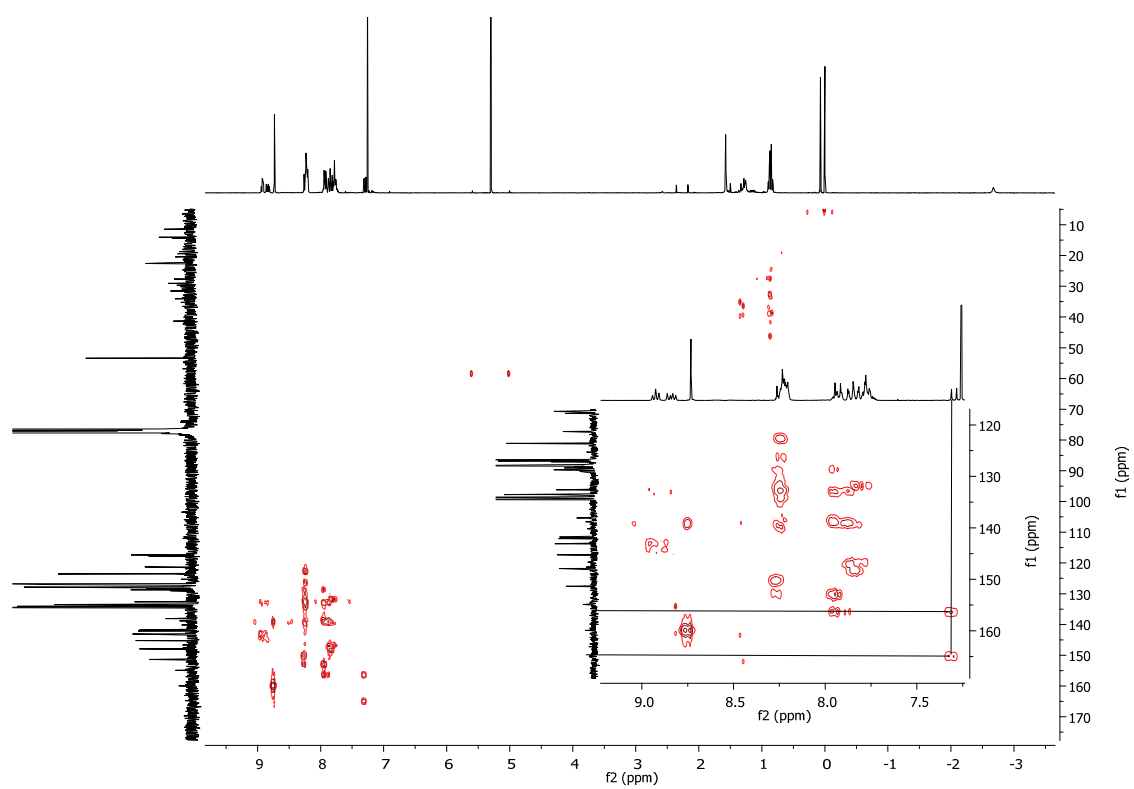


Figure S11 – HMBC spectrum of compound 2d.

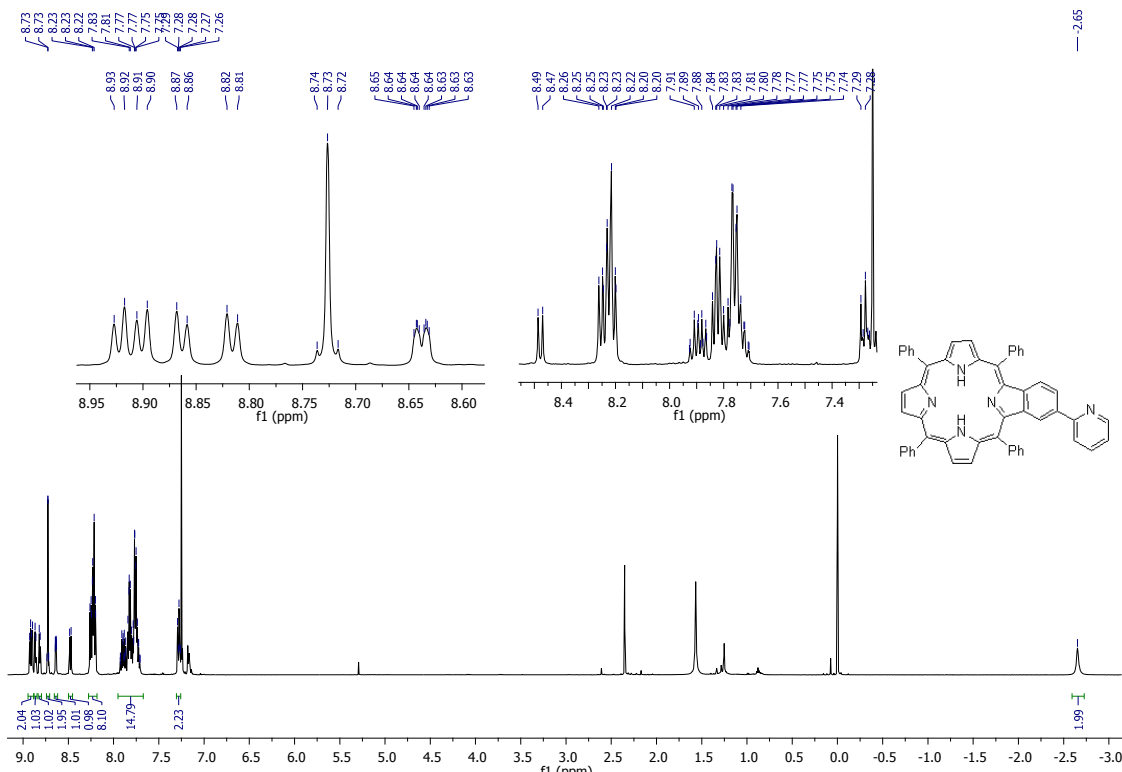


Figure S12 – ^1H NMR spectrum of compound 2e.

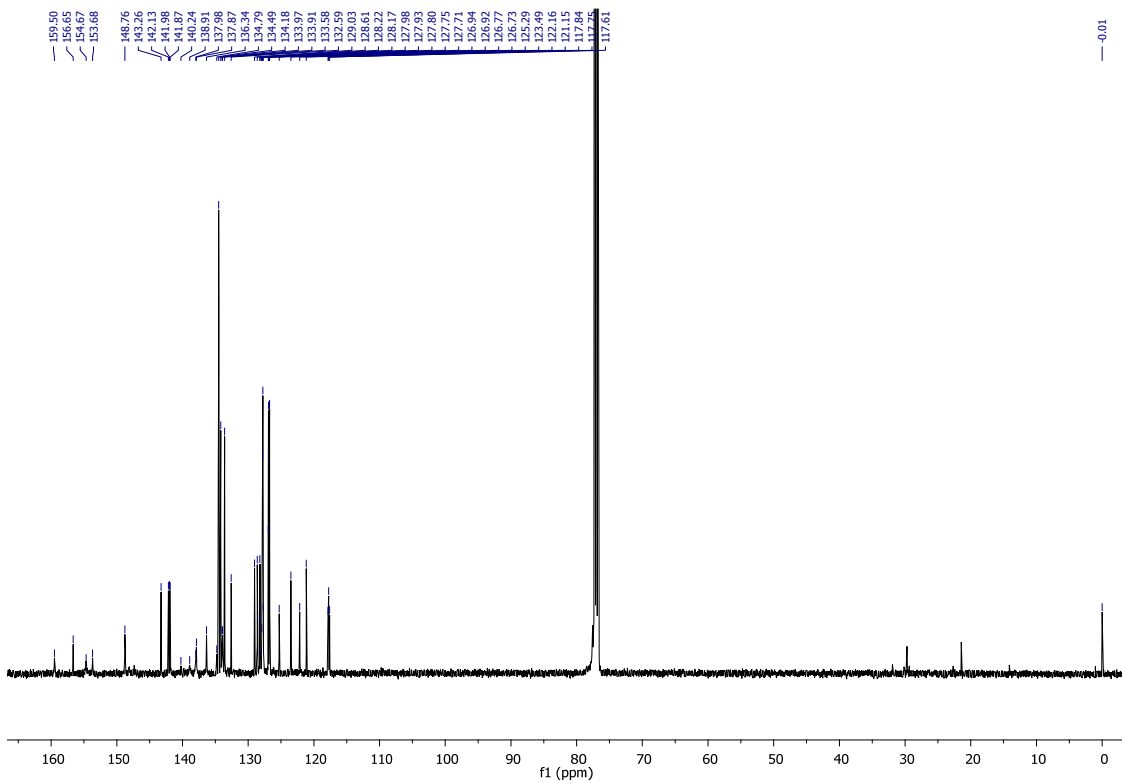


Figure S13 – ^{13}C NMR spectrum of compound 2e.

➤ Compounds 3a-e:

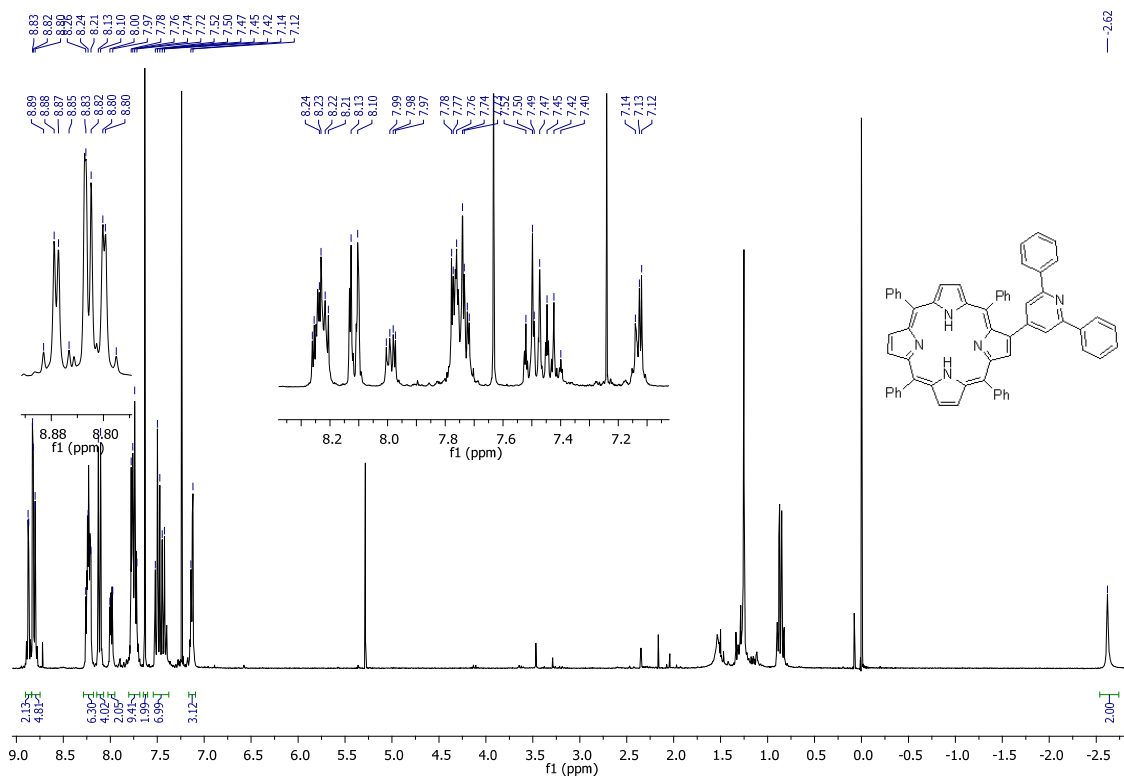


Figure S14 – ^1H NMR spectrum of compound 3a.

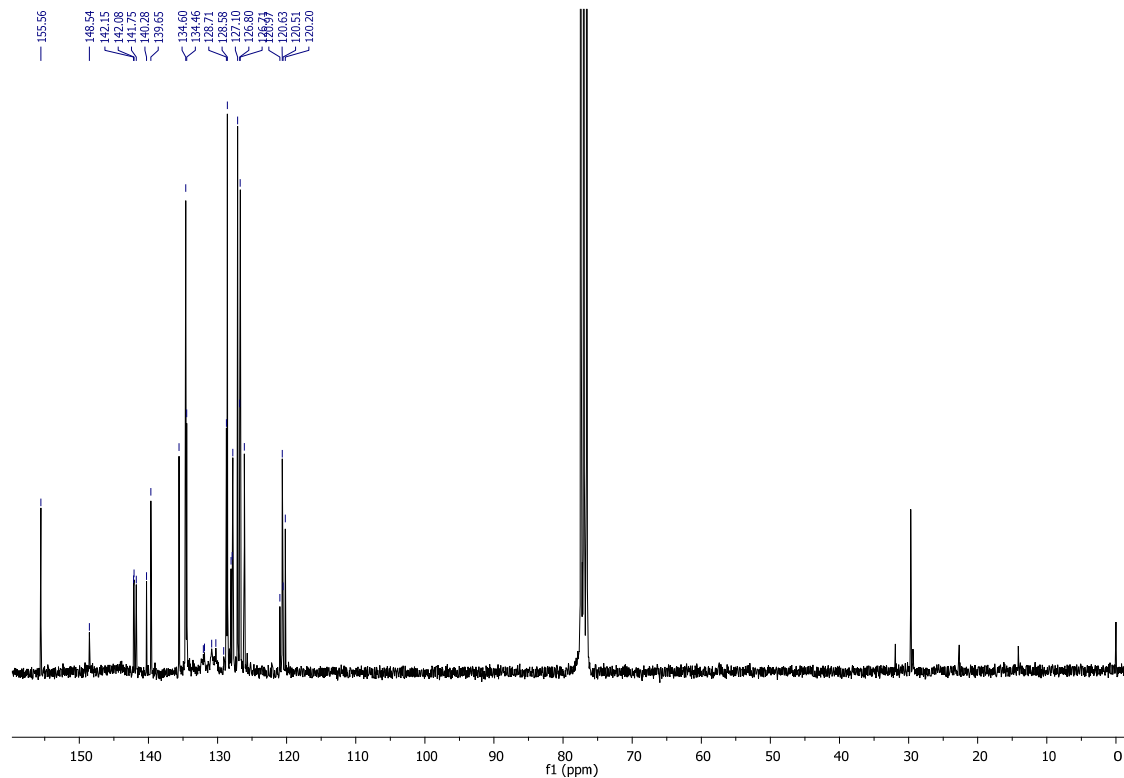


Figure S15 – ^{13}C NMR spectrum of compound 3a.

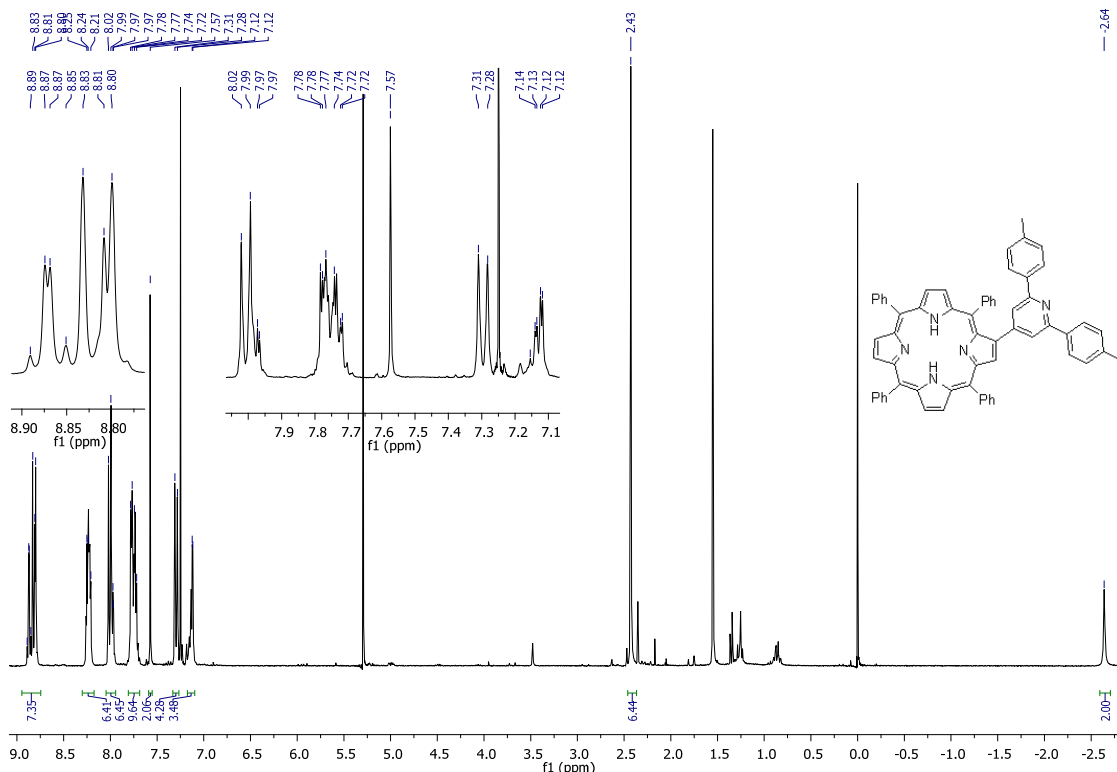


Figure S16 – ¹H NMR spectrum of compound 3b.

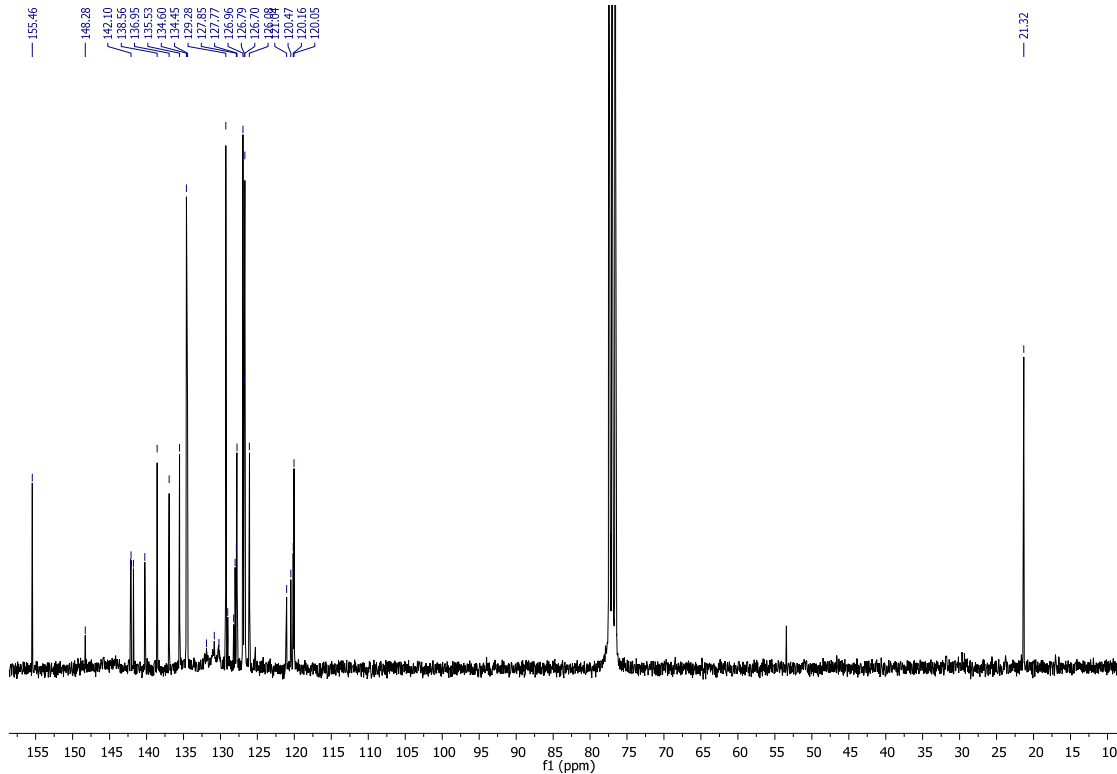


Figure S17 – ¹³C NMR spectrum of compound 3b.

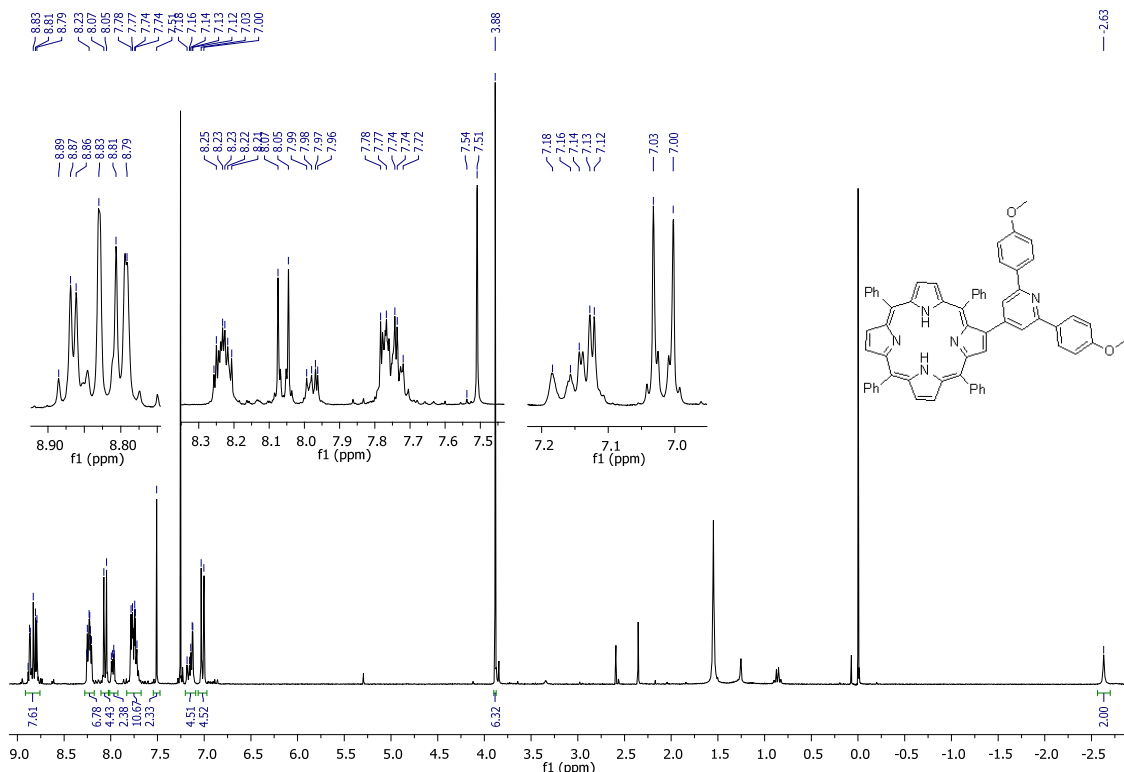


Figure S18 – ¹H NMR spectrum of compound 3c.

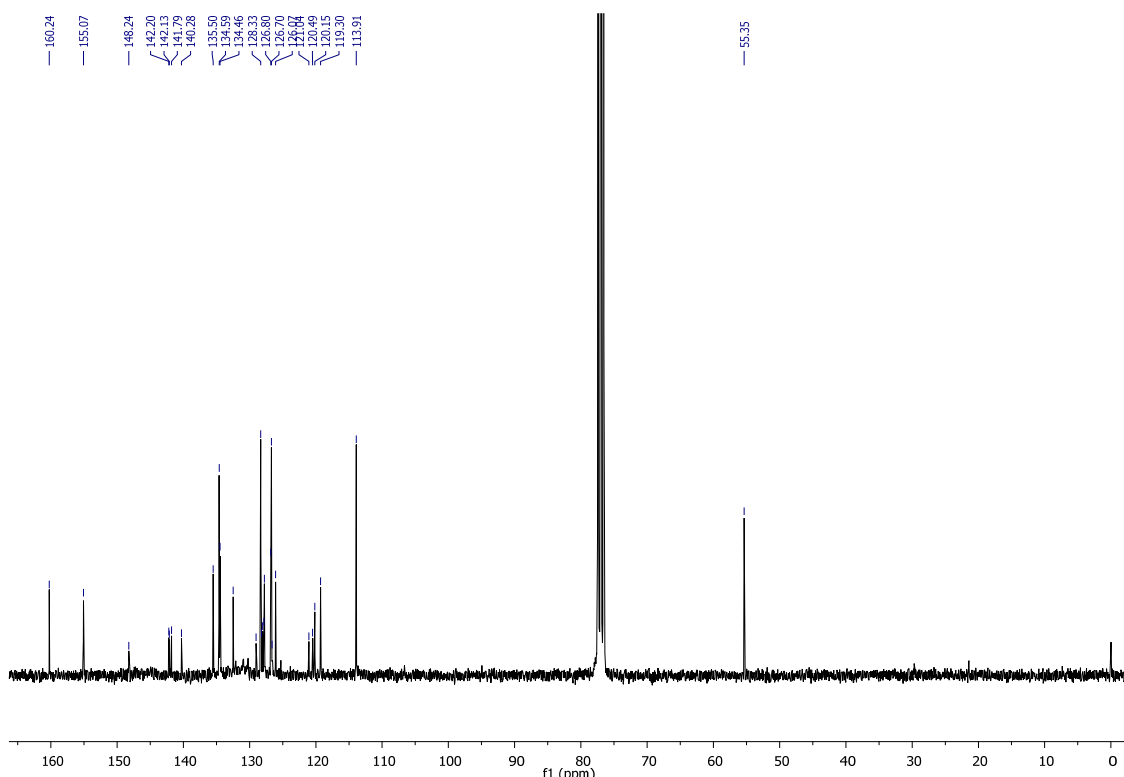


Figure S19 – ¹³C NMR spectrum of compound 3c.

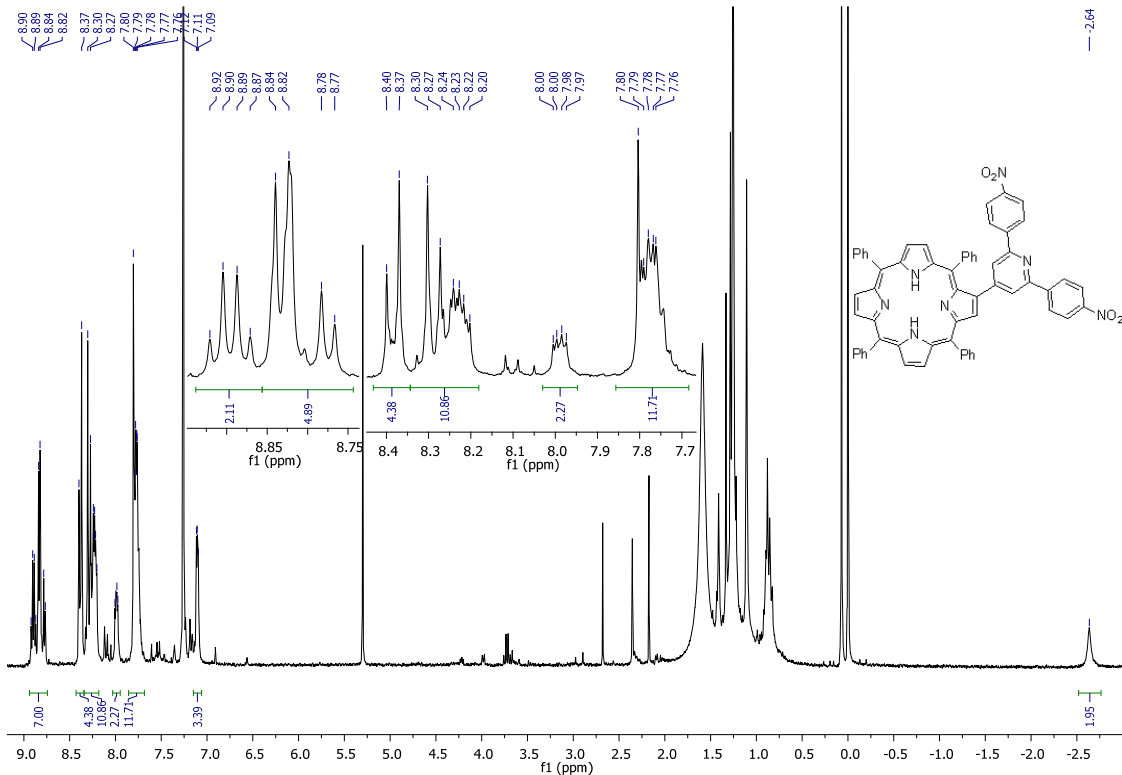


Figure S20 – ^1H NMR spectrum of compound 3d.

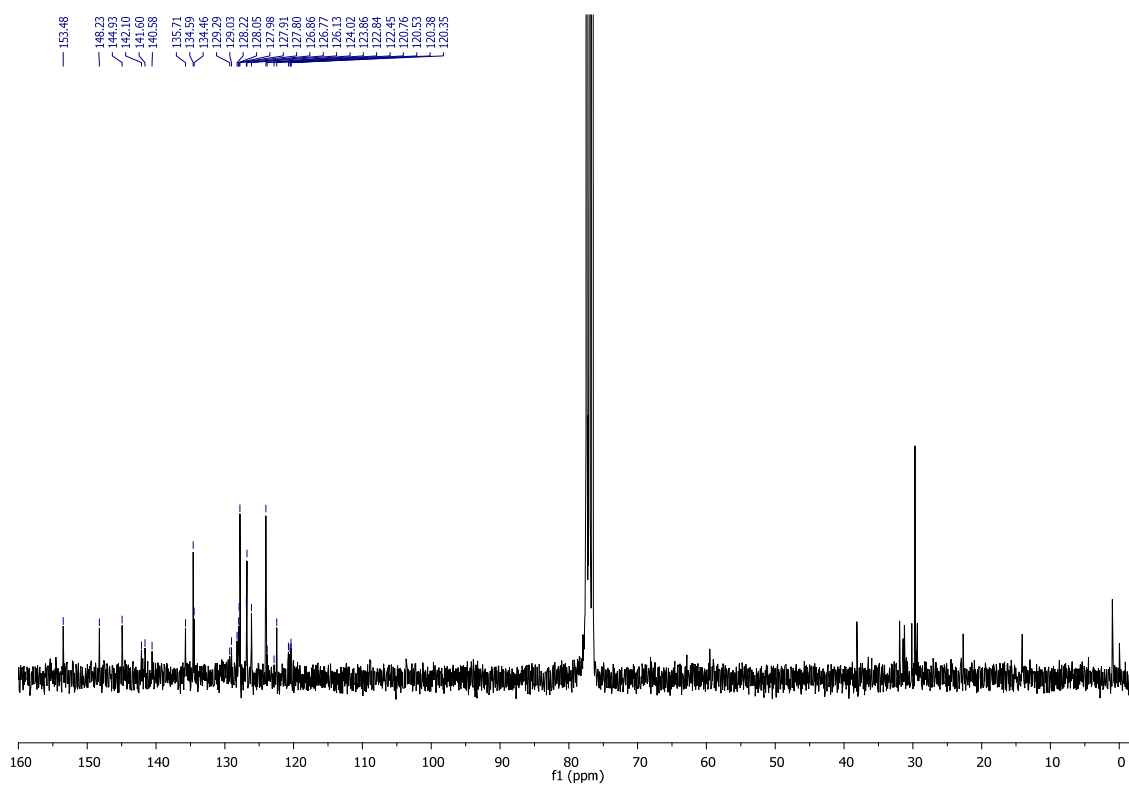


Figure S21 – ^{13}C NMR spectrum of compound 3d.

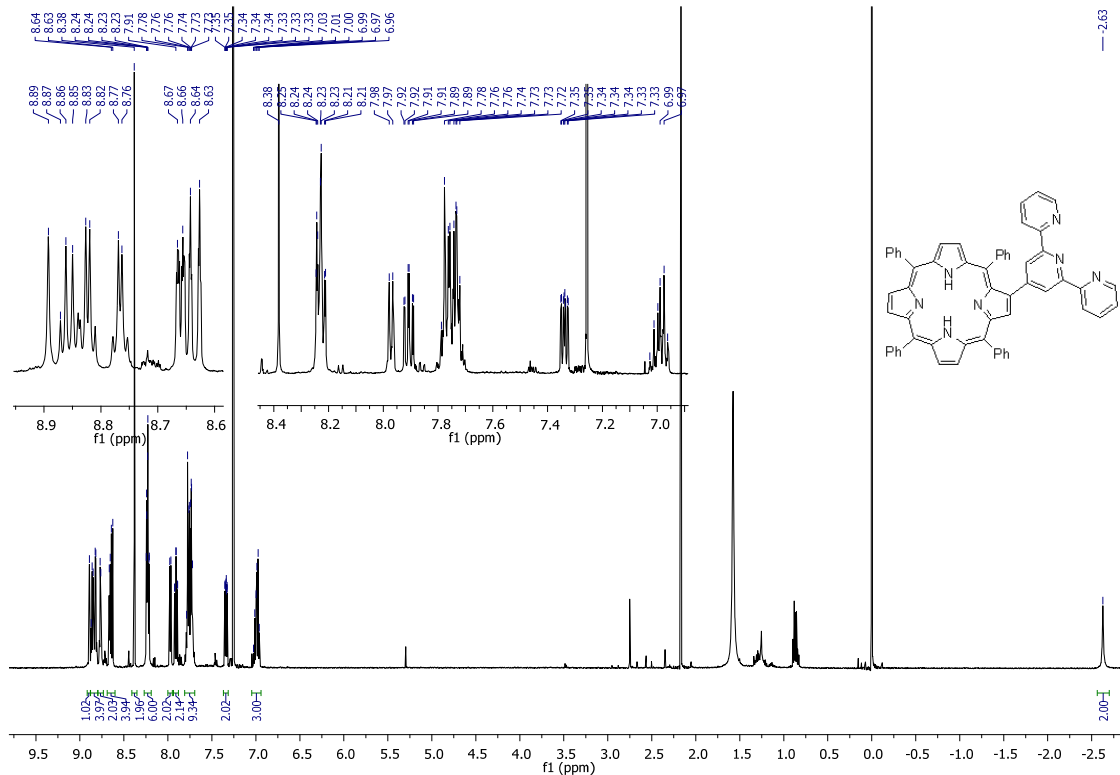


Figure S22 – ¹H NMR spectrum of compound 3e.

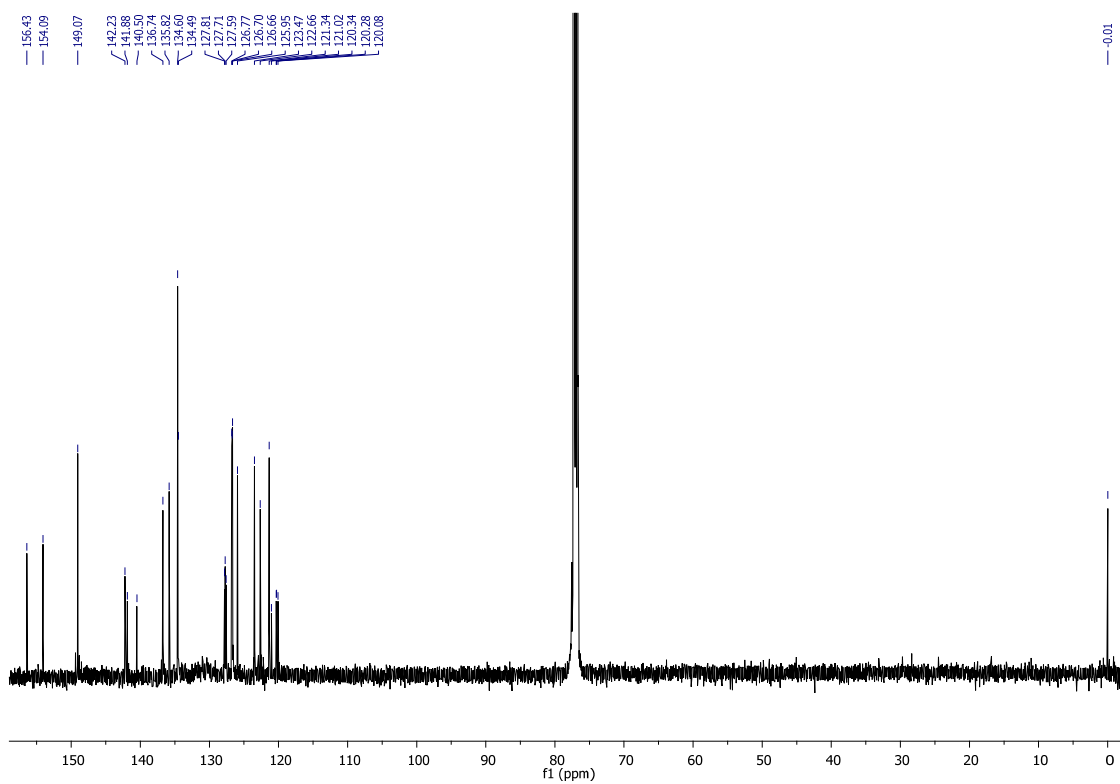


Figure S23 – ¹³C NMR spectrum of compound 3e.

➤ Compounds 4c-e

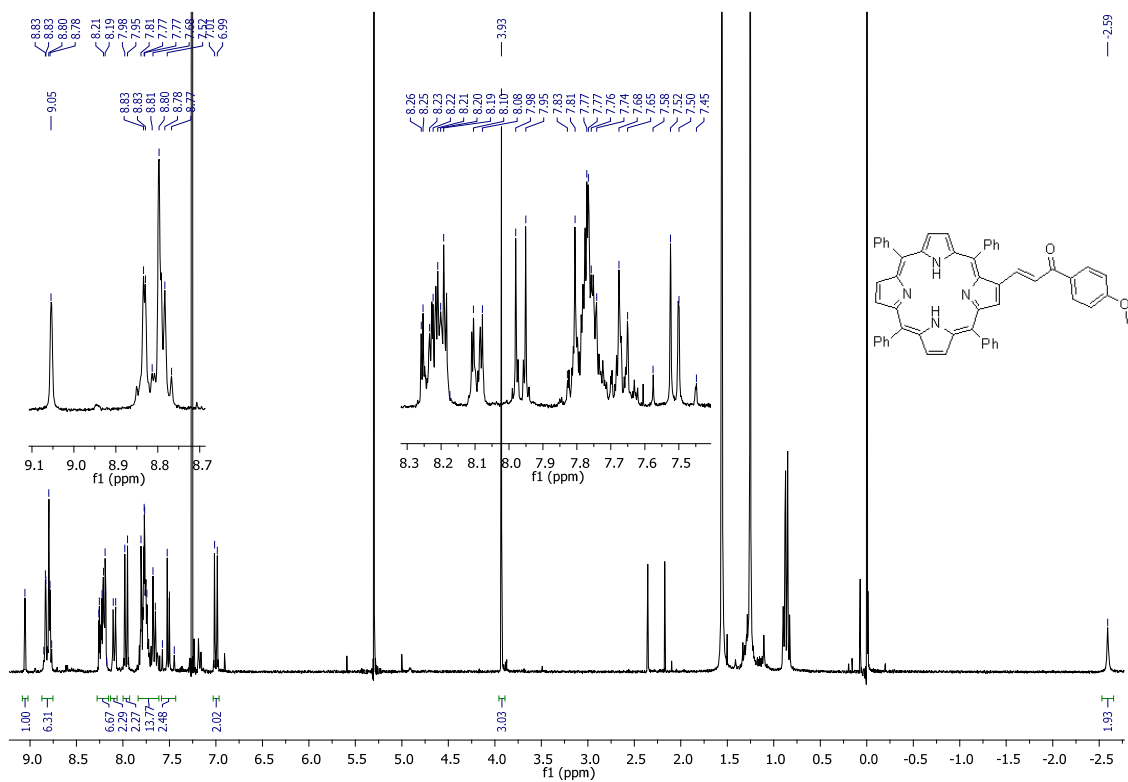


Figure S24 – ^1H NMR spectrum of compound 4c.

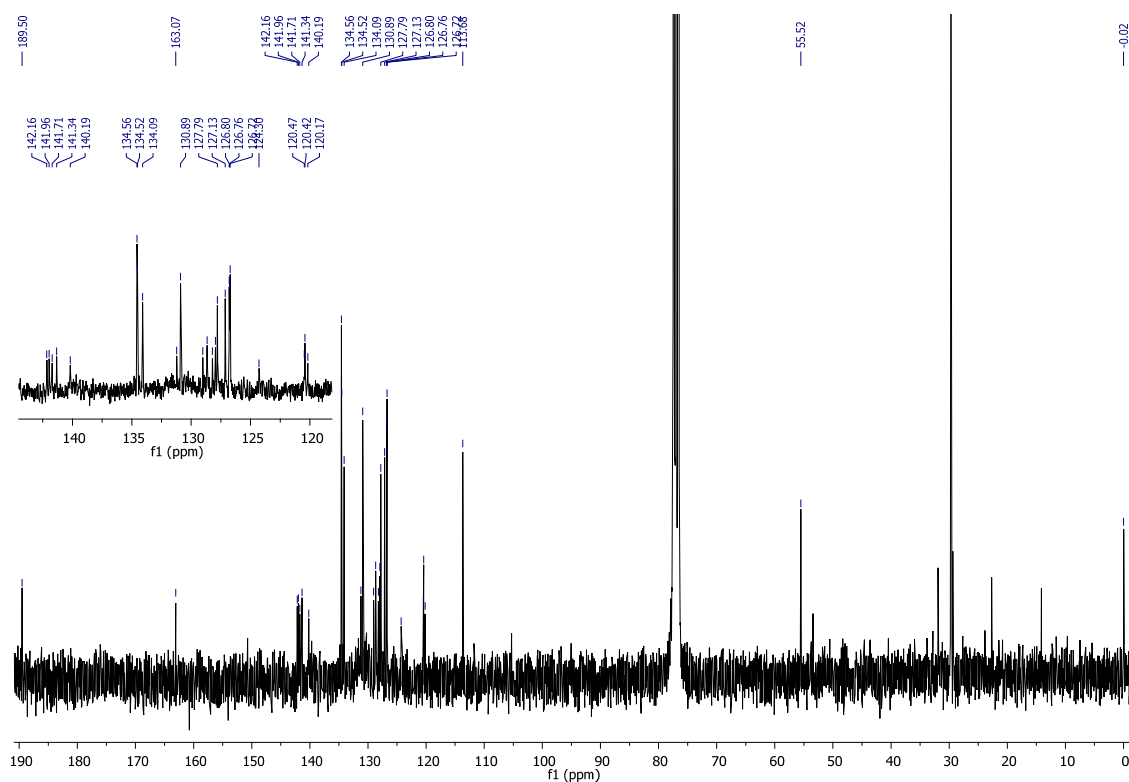


Figure S25 – ^{13}C NMR spectrum of compound 4c.

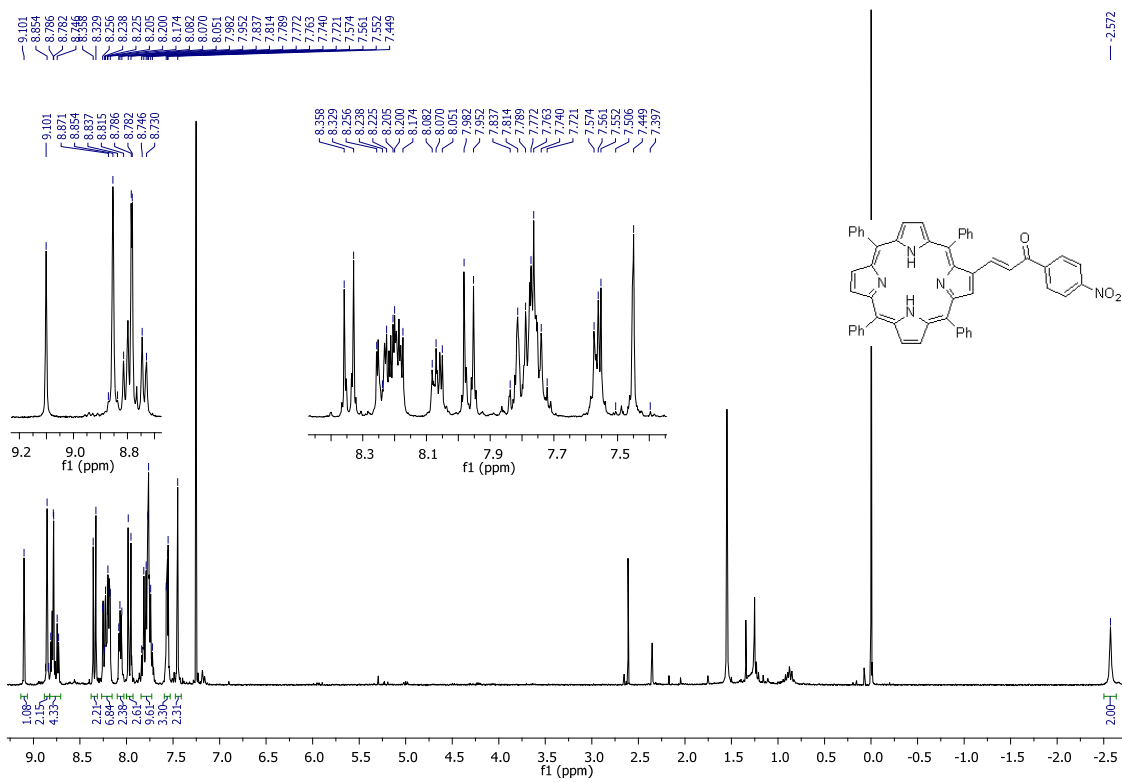


Figure S26 – ^1H NMR spectrum of compound 4d.

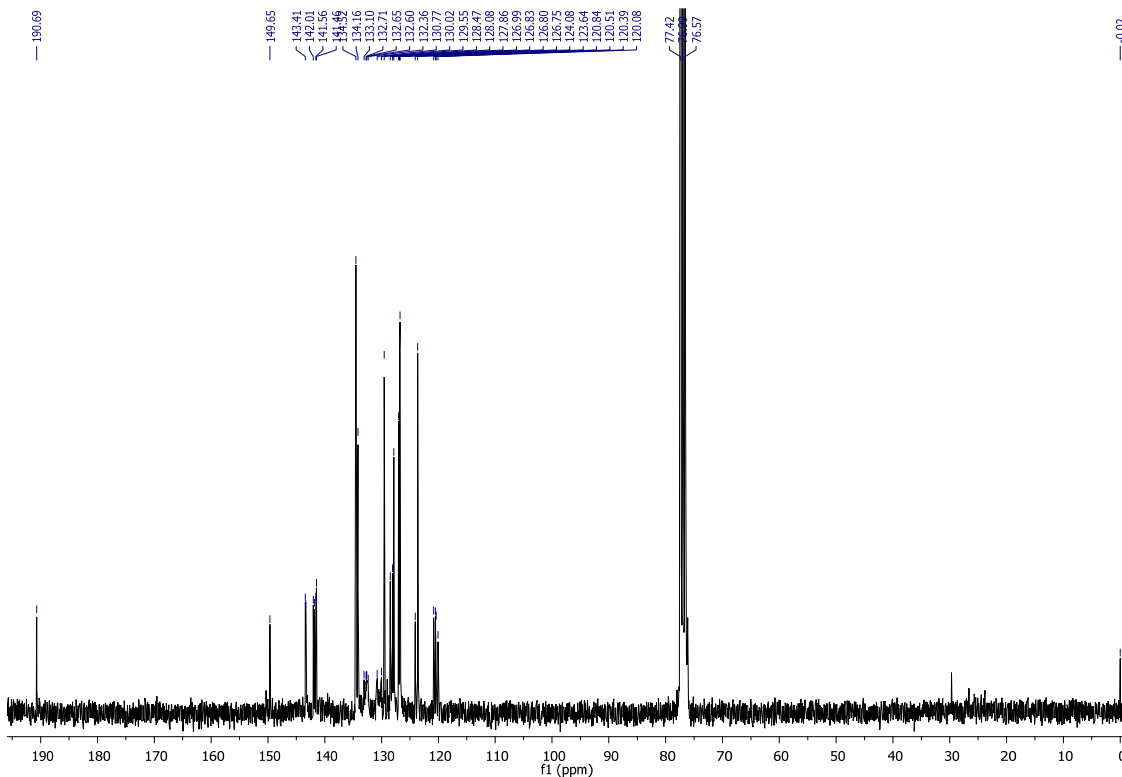


Figure S27 – ^{13}C NMR spectrum of compound 4d.

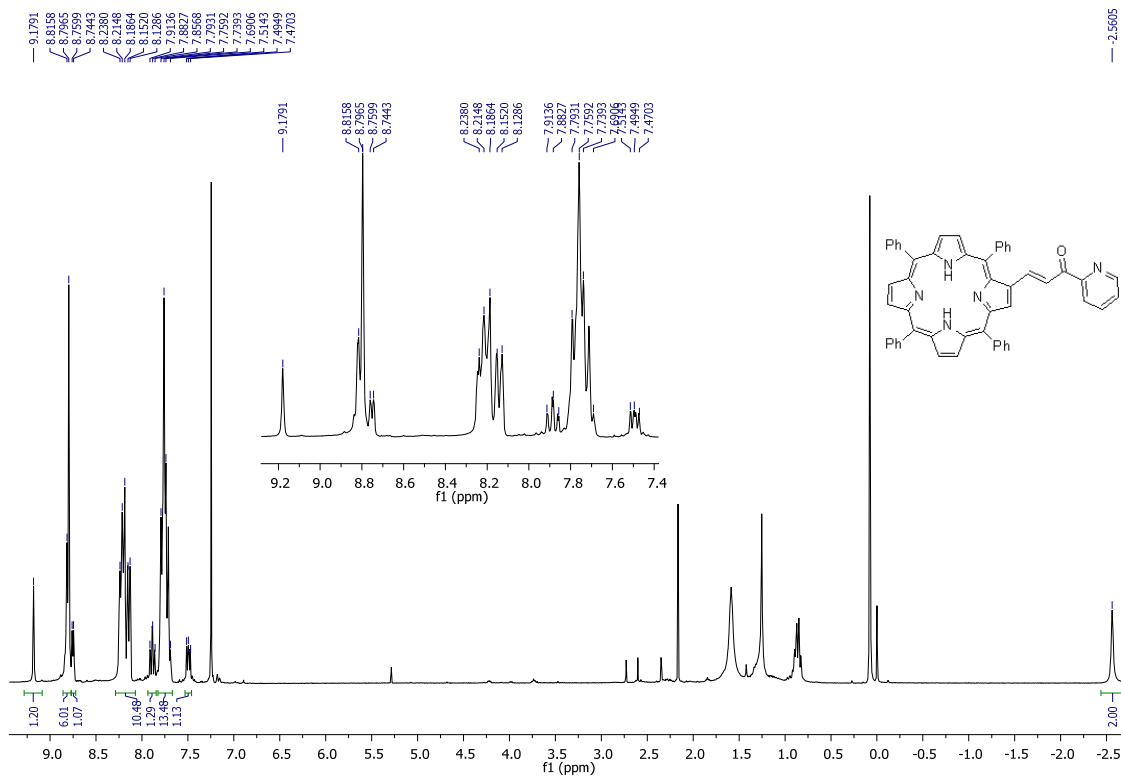


Figure S28 – ¹H NMR spectrum of compound 4e.

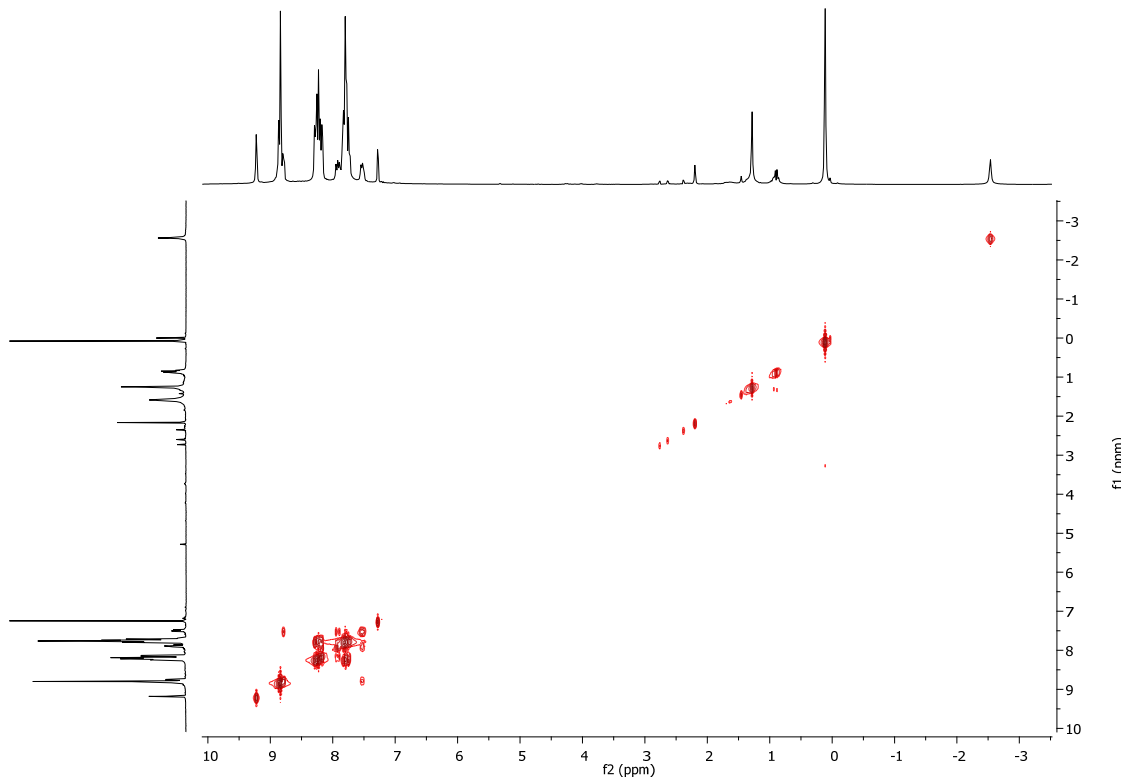


Figure S29 – COSY spectrum of compound 4e.

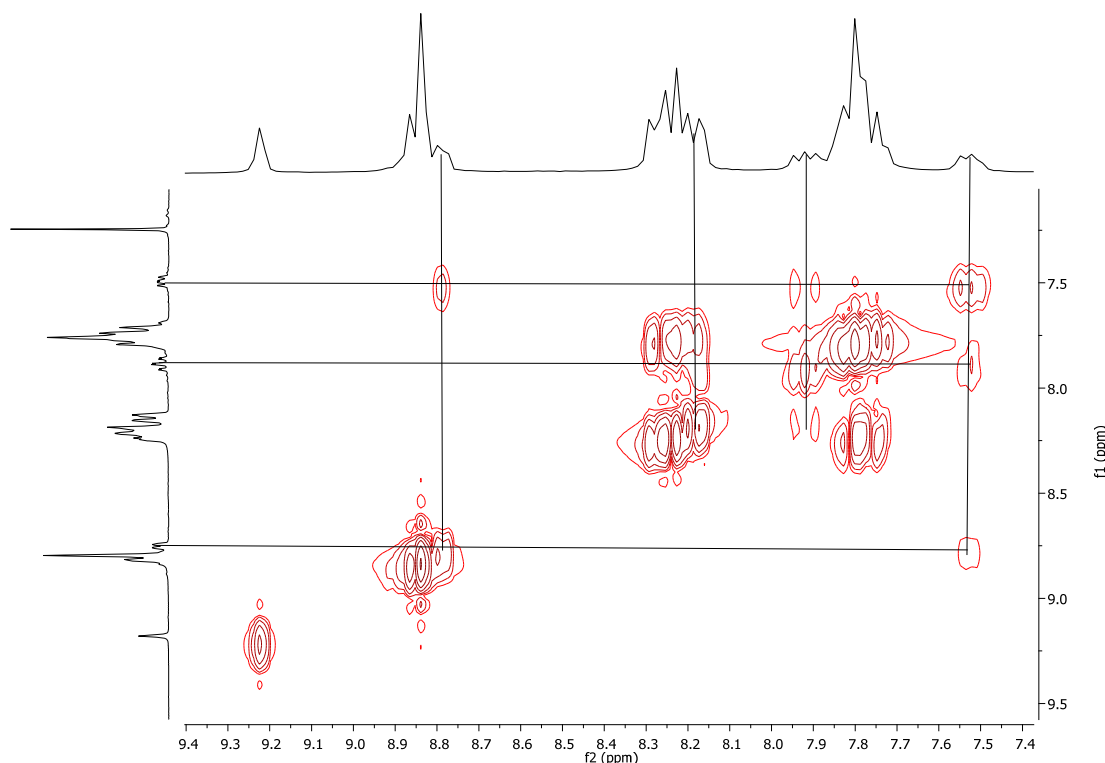


Figure S30 – Partial COSY spectrum of compound 4e.

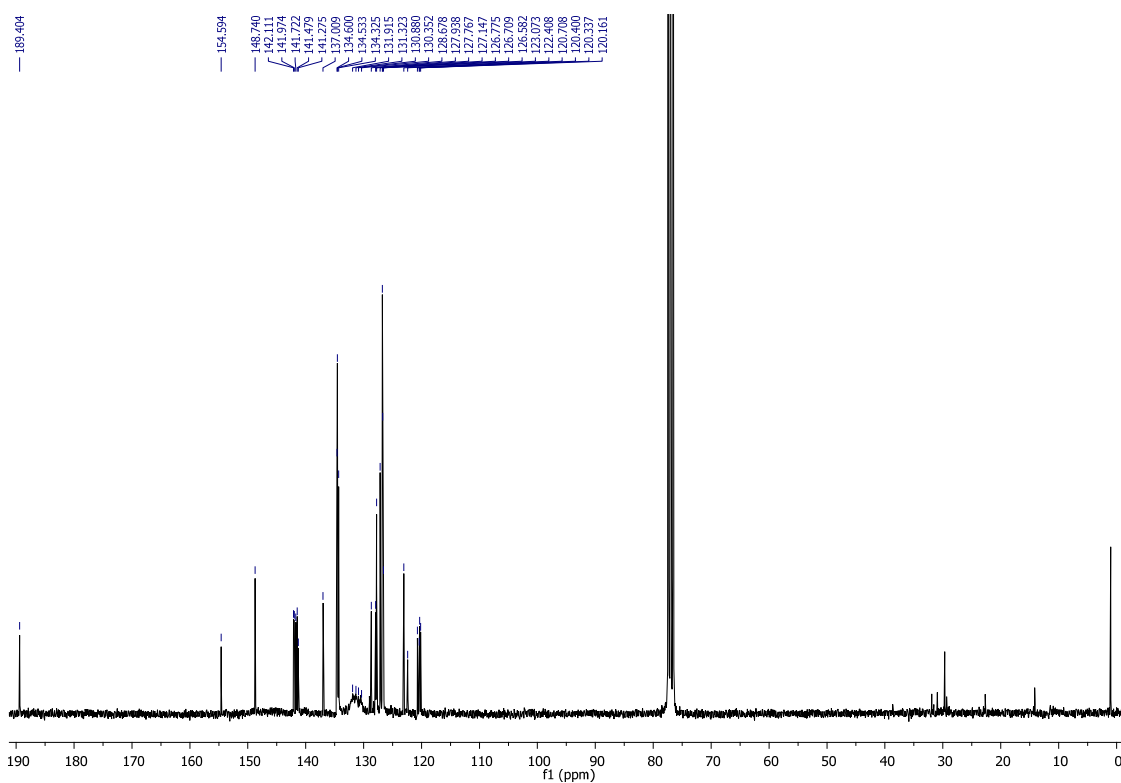


Figure S31 – ^{13}C NMR spectrum of compound 4e.

➤ Compound 5:

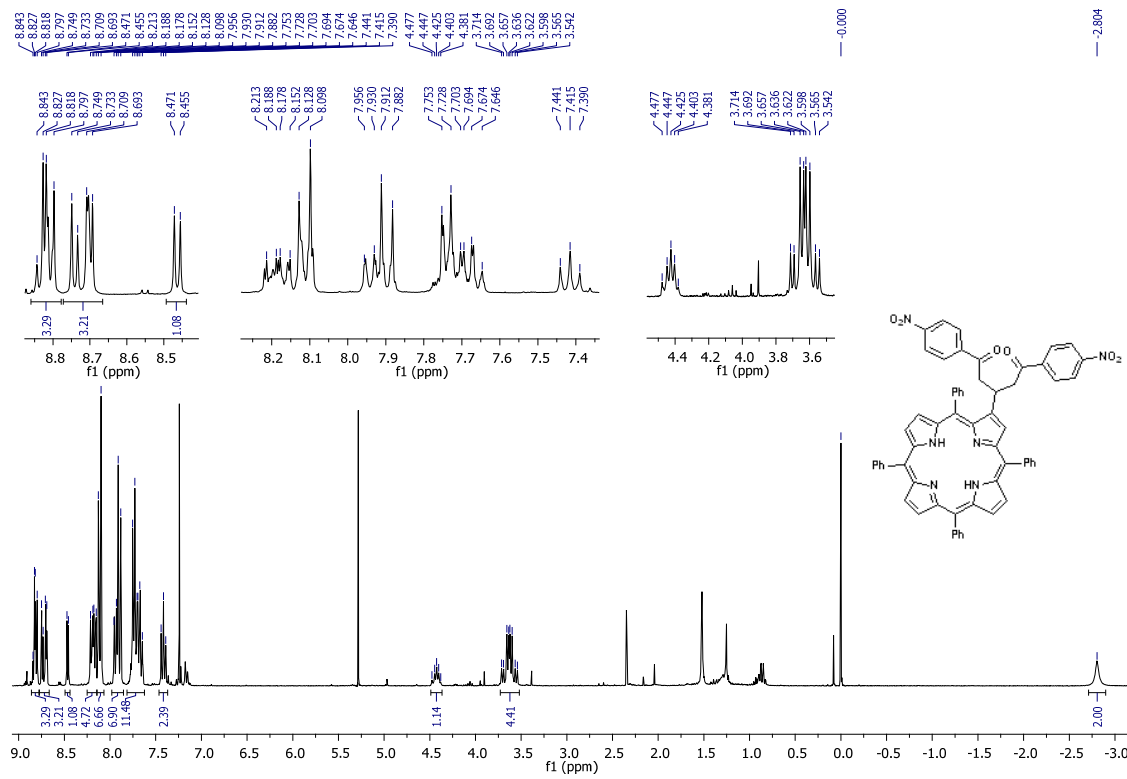


Figure S32 – ^1H NMR spectrum of compound 5.

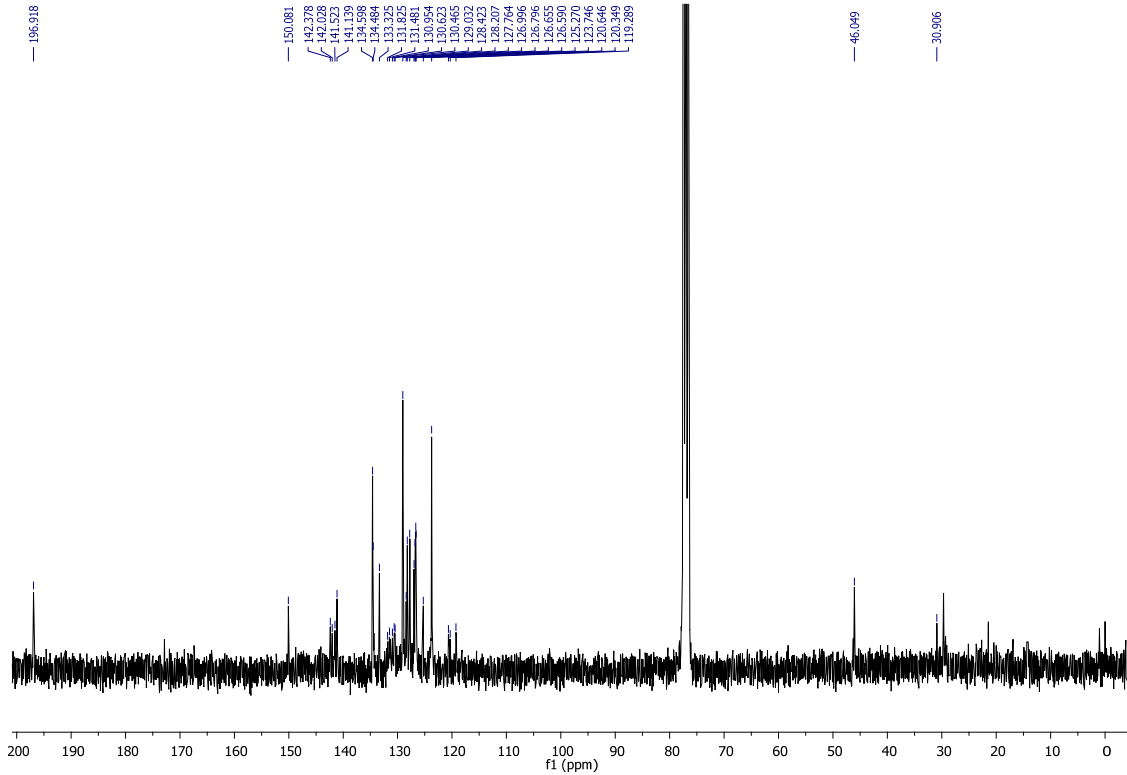


Figure S33 – ^{13}C NMR spectrum of compound 5.

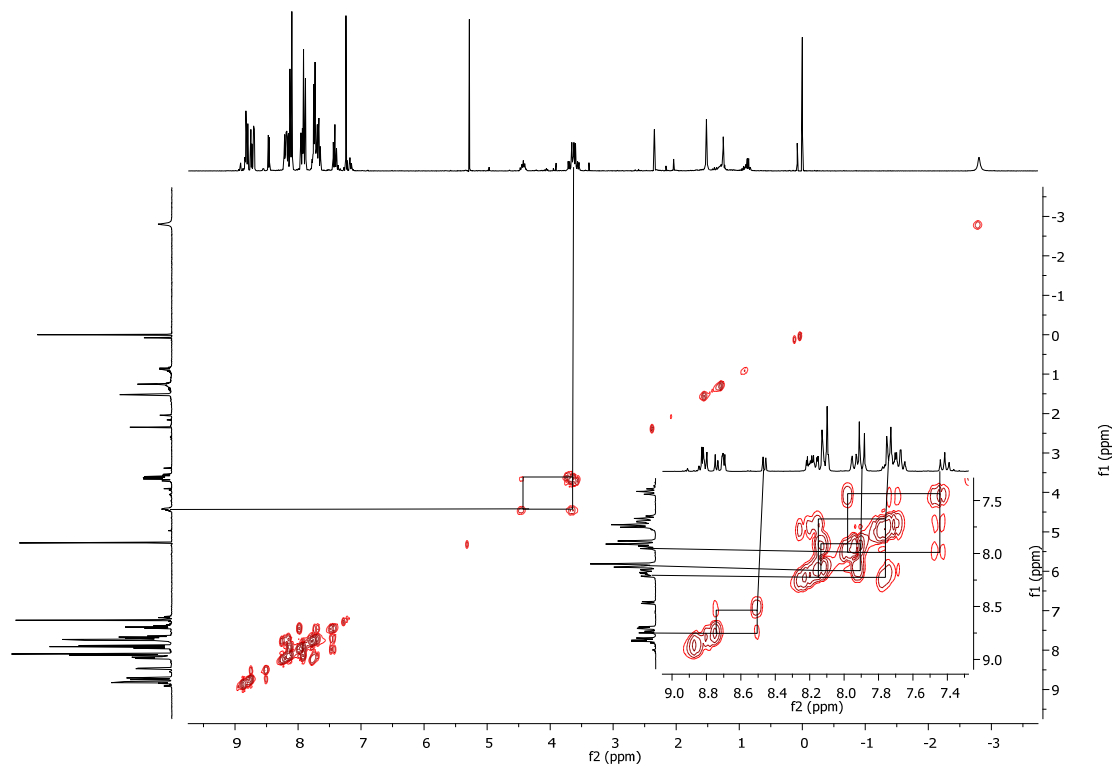


Figure S34 – COSY Spectrum of compound 5.

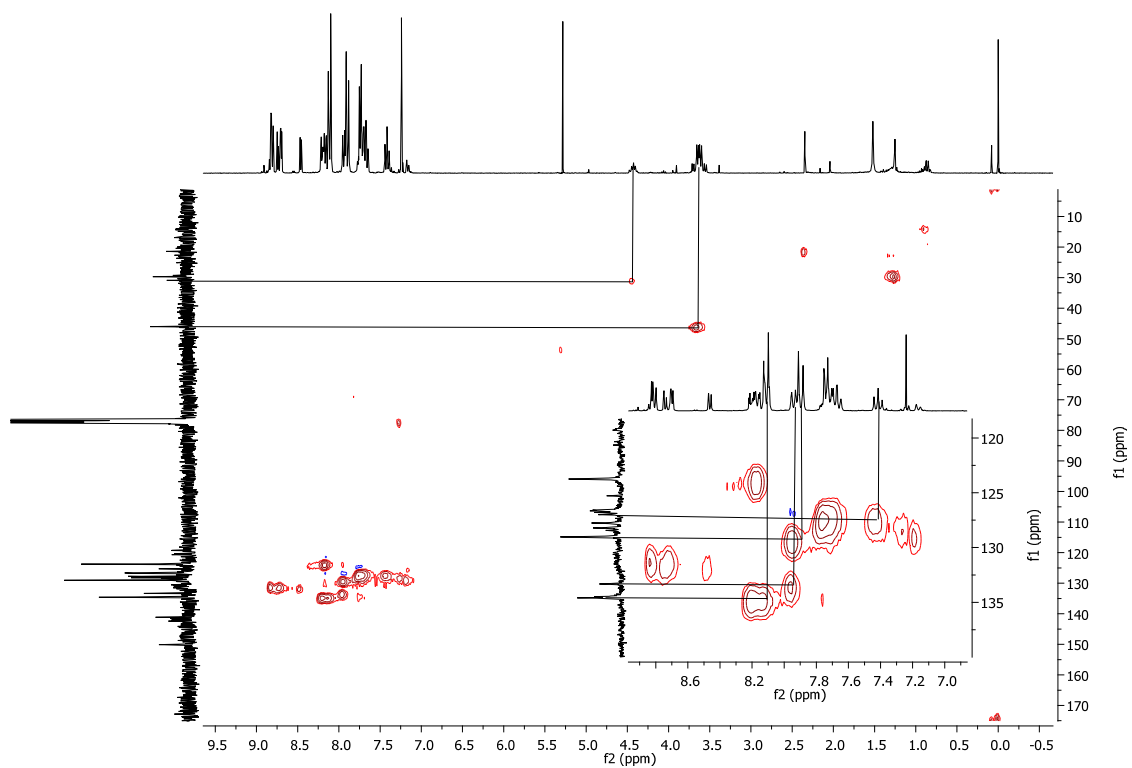


Figure S35– HSQC NMR spectrum of compound 5.

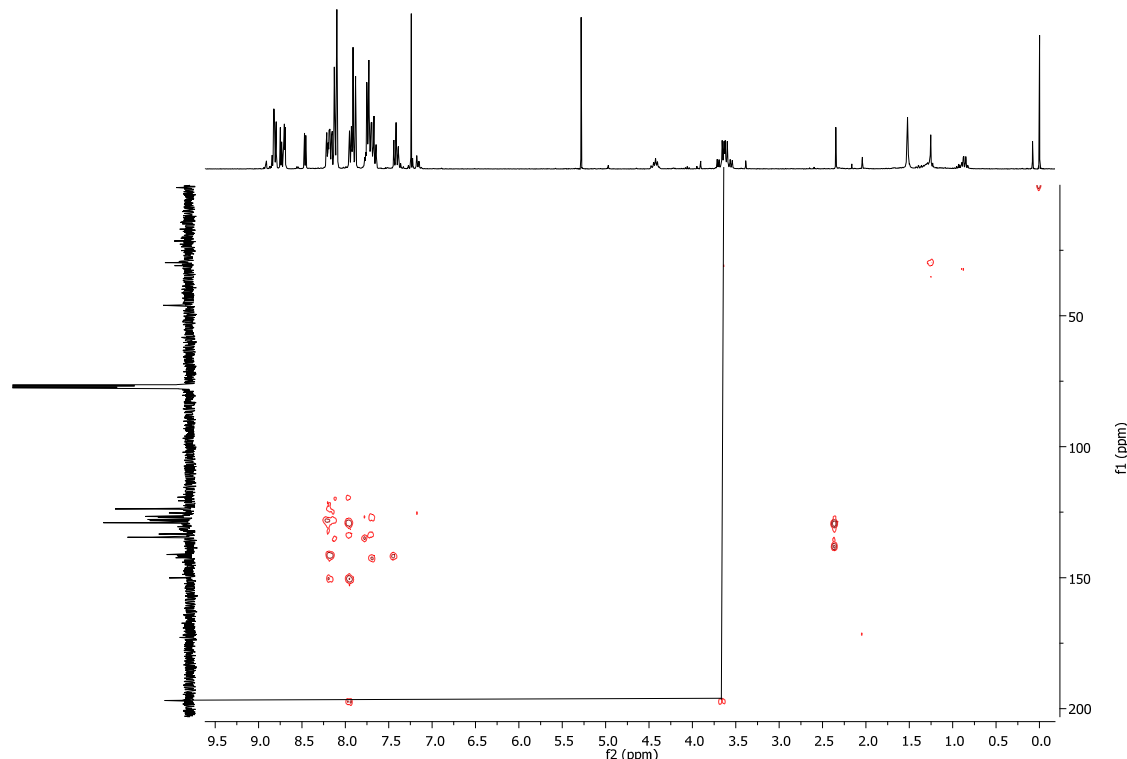


Figure S36 – HMBC NMR spectrum of compound 5.

V - Single-Crystal X-ray Diffraction Studies

Single-crystals of compounds **3b** and **3e** were manually harvested from the crystallization vials and mounted on either Hampton Research CryoLoops (using FOMBLIN Y perfluoropolyether vacuum oil (LVAC 140/13) purchased from Sigma-Aldrich),³ with the help of a Stemi 2000 stereomicroscope equipped with Carl Zeiss lenses, or on glass fibres. Data were collected at 150(2) K on a Bruker X8 Kappa APEX II charge-coupled device (CCD) area-detector diffractometer (Mo K α graphite-monochromated radiation, $\lambda = 0.71073 \text{ \AA}$) controlled by the APEX2 software package,⁴ and equipped with an Oxford Cryosystems Series 700 cryostream monitored remotely using the software interface Cryopad.⁵ Images were processed using the software package SAINT+,⁶ and data were corrected for absorption by the multi-scan semi-empirical method implemented in SADABS.⁷

The crystal structures were solved by employing the direct methods algorithm implemented in the software package SHELXS-97.^{8, 9} This approach allowed the immediate location of the majority of the non-hydrogen atoms composing the molecular units of **3b** and **3e**. All remaining non-hydrogen atoms were directly located from difference Fourier maps calculated from successive full-matrix least squares refinement cycles on F^2 using SHELXL-97.^{9, 10} In general, non-hydrogen atoms have been successfully refined using anisotropic displacement parameters (the exceptions for **3e** are detailed below).

In compound **3e**, the two peripheral pyridine aromatic rings belonging to the terpyridine substituent were found to be severely affected by a combination of thermal and positional disorder. The molecular unit of this compound was ultimately modelled by assuming that the central pyridine ring is common to the various possible structural conformations and by fixing two distinct locations for each peripheral pyridine ring with a rate of occupancy of 0.50 each (please note: this value was approximately derived from unrestrained refinement for the respective site occupancies). Due to the considerable smeared-out electron density associated with this moiety, the geometry of these peripheral aromatic rings had to be significantly restrained to provide an overall stable refinement, by employing the *AFIX 66* instruction to standardise the bond lengths of the aromatic rings. In addition, for each pyridine ring, all atoms were refined while assuming a common (and refineable) isotropic displacement parameter (one for each pyridine ring). The location of the nitrogen atoms belonging to the peripheral pyridine aromatic rings was unequivocally derived from geometrical reasons concerned with the various possible supramolecular contacts which may indeed exist in the crystal structure which involve these moieties. In fact, we believe that the considerable structural disorder observed for this molecule arises exactly from the similar orientation of all nitrogen atoms towards to inner space of the terpyridine moiety, creating a considerable steric hindrance associated with the non-bonding electron pairs of these atoms and, consequently, promoting the rotation of the aromatic rings so to minimize repulsion.

Besides the molecular units of **3e**, the actual crystal structure contains several inner voids (total volume of about 299 Å³ as estimated by PLATON),^{11, 12} distributed among four cavities with the largest being centred at (0 0 0) and (0 0.5 0), which most likely contain highly disordered solvent molecules. From difference Fourier maps it was possible to discern the presence of a considerable smeared-out electron density in these locations. Nevertheless, a number of attempts to locate and model solvent molecules proved to be unproductive. The original data set was treated using the *SQUEEZE*¹³ subroutines implemented in PLATON^{11, 12} in order to remove the contribution of these highly disordered molecules. It was estimated that the aforementioned cavities would contain a total of *ca.* 82 electrons. The calculated solvent-free reflection list was used for subsequent structural refinements which converged to the solvent-free structure reported in this manuscript and having the reliability factors summarised in the main manuscript.

Despite the location of most of the hydrogen atoms bound to carbon and nitrogen could be discerned from difference Fourier maps at the later stages of the refinement procedure, these were instead placed at idealised positions using the *HFIX 43* or *137* instructions in SHELXL (for the aromatic and terminal -CH₃ moieties, respectively), and included in subsequent

refinement cycles in riding-motion approximation with U_{iso} fixed at 1.2 or $1.5 \times U_{\text{eq}}$ of the carbon atom to which they are attached, respectively.

The last difference Fourier map synthesis showed: for **3b**, the highest peak ($0.255 \text{ e}\text{\AA}^{-3}$) and deepest hole ($-0.300 \text{ e}\text{\AA}^{-3}$) located at 0.88 \AA and 1.07 \AA from N3 and C62, respectively; for **3e** (using the SQUEEZE data), the highest peak ($0.793 \text{ e}\text{\AA}^{-3}$) and deepest hole ($-0.377 \text{ e}\text{\AA}^{-3}$) located at 0.92 \AA and 0.43 \AA from H60' and N61, respectively.

Crystallographic data (including structure factors) for the structures reported in this paper have been deposited with the Cambridge Crystallographic Data Centre as supplementary publication nos. CCDC-859837 (for **3b**) and -859838 (for **3e**). Copies of the data can be obtained free of charge on application to CCDC, 12 Union Road, Cambridge CB2 2EZ, U.K. FAX: (+44) 1223 336033. E-mail: deposit@ccdc.cam.ac.uk.

Crystallographic Tables

Compound 3b

Table S1. Supramolecular contacts present in compound **3b**. Distances are given in Å and interaction angles in degrees.^{a,b}

D–H···A	d(D···A)	∠(DHA)
C38–H38···Cg ₁ ⁱ	3.338(4)	122
C40–H40···Cg ₂ ⁱ	3.761(4)	150
C42–H42···Cg ₃ ⁱⁱ	3.562(4)	129
π-π Contacts		<i>Inter-centroid distance</i>
Cg ₄ ···Cg ₅	3.693(2)	
Cg ₄ ···Cg ₆ ⁱⁱⁱ	3.978(2)	

^a Symmetry transformations used to generate equivalent atoms:
(i) 1-x, 1-y, 2-z; (ii) 1-x, 2-y, 1-z; (iii) 1-x, 1-y, 1-z.

^b Centres of gravity (Cg) (see Figure S1):

Cg₁ = N2, C6, C7, C8 and C9;

Cg₂ = C27, C28, C29, C30, C31 and C32;

Cg₃ = C57, C58, C59, C60, C61 and C62;

Cg₄ = N5, C45, C46, C47, C49 and C50;

Cg₅ = C39, C40, C41, C42, C43 and C44;

Cg₆ = C51, C52, C53, C54, C55 and C56.

Compound 3e

Table S2. Supramolecular contacts present in compound 3e. Distances are given in Å and interaction angles in degrees.^{a,b}

D–H···A	d(D···A)	∠(DHA)
C29–H29···Cg ₁ ⁱ	3.713(7)	143
C31–H31···Cg ₂ ⁱⁱ	3.465(7)	132
C37–H37···Cg ₃ ⁱⁱⁱ	3.865(8)	157
C43–H43···Cg ₄ ^{iv}	3.716(7)	138

π-π Contacts	<i>Inter-centroid distance</i>
Cg ₅ ···Cg ₆	3.521(3)

^a Symmetry transformations used to generate equivalent atoms:

(i) 2-x, 1-y, 1-z; (ii) 3-x, 1-y, 1-z; (iii) 3-x, 2-y, 1-z; (iv) 2-x, 2-y, 1-z.

^b Centres of gravity (Cg) (see Figure S4):

Cg₁ = N1, C1, C2, C3 and C4;

Cg₂ = N4, C16, C17, C18 and C19;

Cg₃ = C39, C40, C41, C42, C43 and C44;

Cg₄ = N3, C11, C12, C13 and C14;

Cg₅ = N5, C45, C46, C47, C48 and C49;

Cg₆ = C21, C22, C23, C24, C25 and C26.

Additional Structural Drawings

Compound 3b

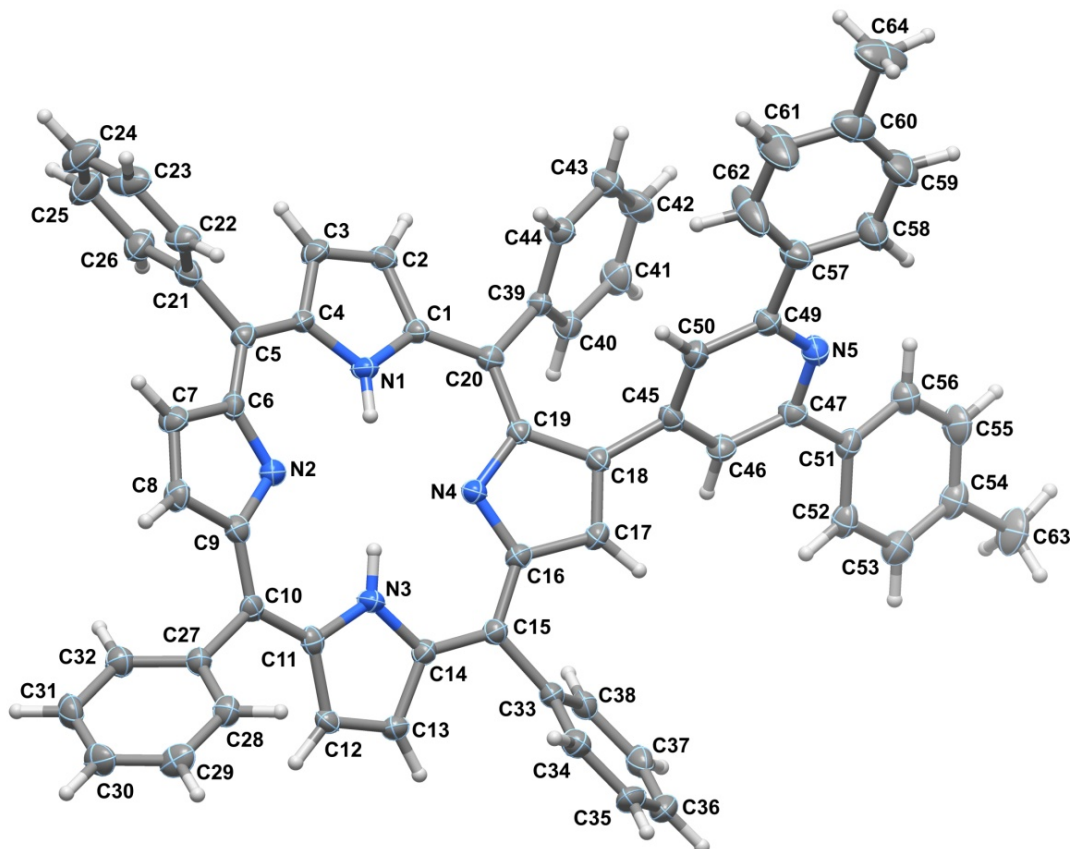


Figure S41. Schematic representation of the molecular unit composing the asymmetric unit of compound **3b**. Non-hydrogen atoms are represented as thermal ellipsoids drawn at the 50% probability level and hydrogen atoms as small spheres with arbitrary radius. The atomic labelling is provided for all non-hydrogen atoms.

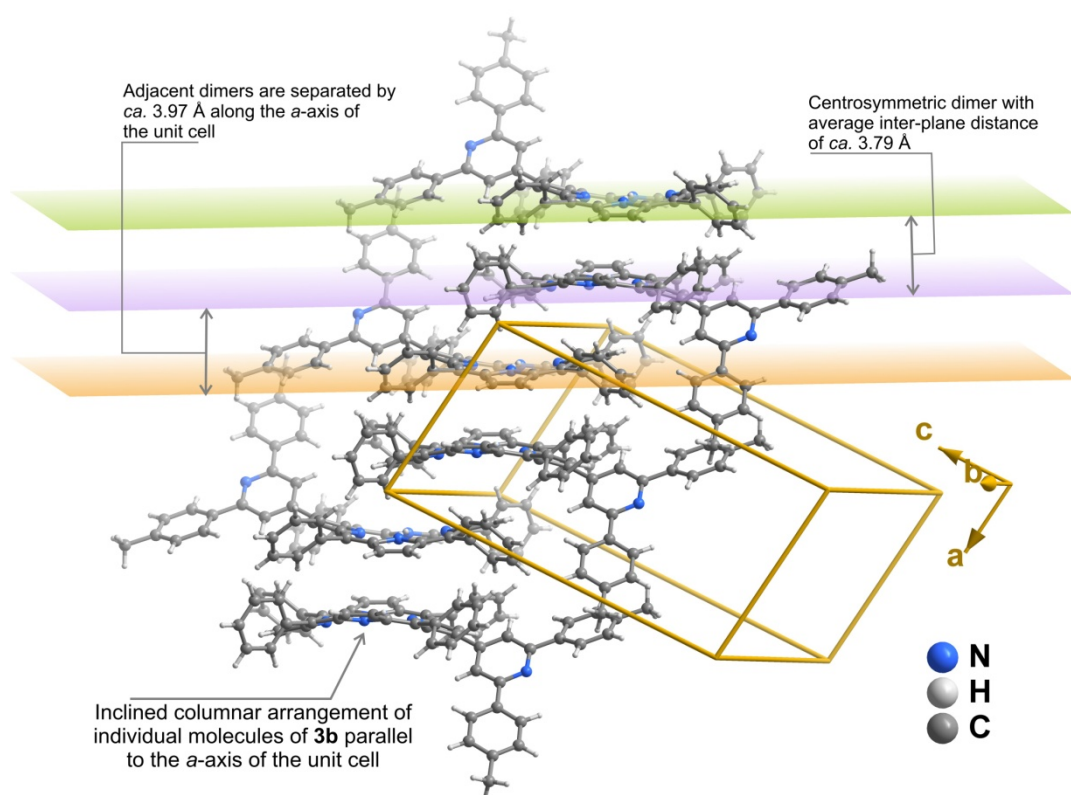


Figure S42. Arrangement of individual molecular units of **3b** forming a supramolecular column parallel to the *a*-axis of the unit cell. The closest inter-planar distance between adjacent molecular units is of ca. 3.79 Å, forming centrosymmetric pseudo-dimers which are, in turn, separated by ca. 3.97 Å along the same direction.

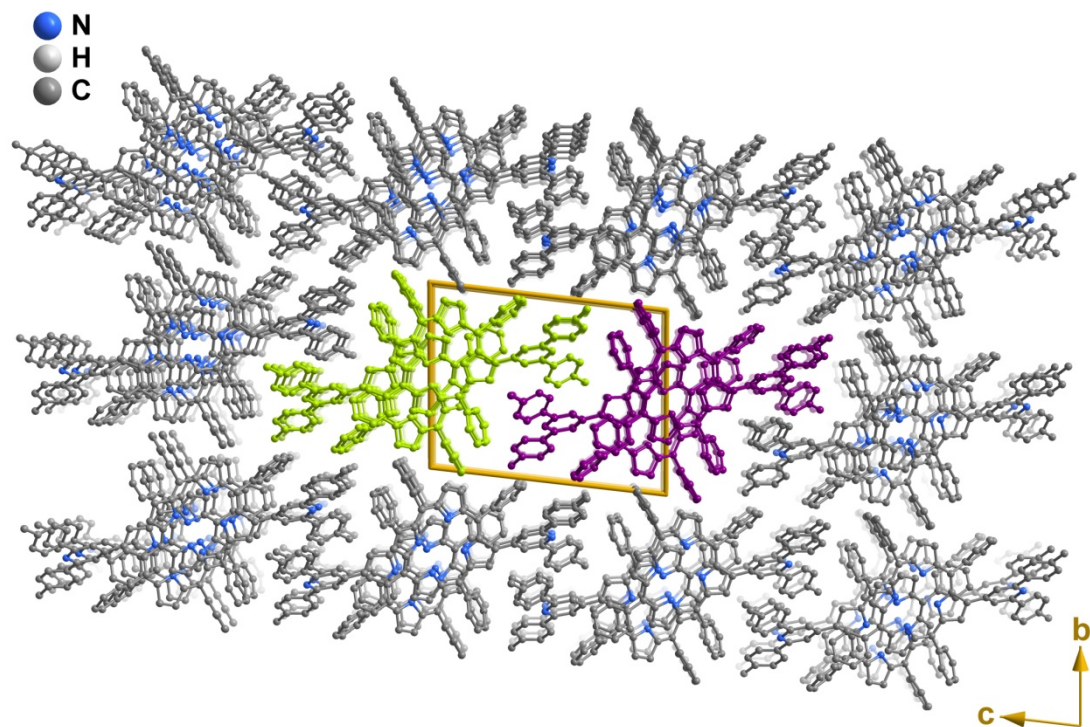


Figure S43. Crystal packing of compound **3b** viewed in perspective along the [100] direction of the unit cell. For clarity, two of the supramolecular columnar arrangements of molecular units of **3b** (as shown in Figure S2) are depicted at the centre of the image in different colour. Hydrogen atoms have been omitted for clarity.

Compound 3e

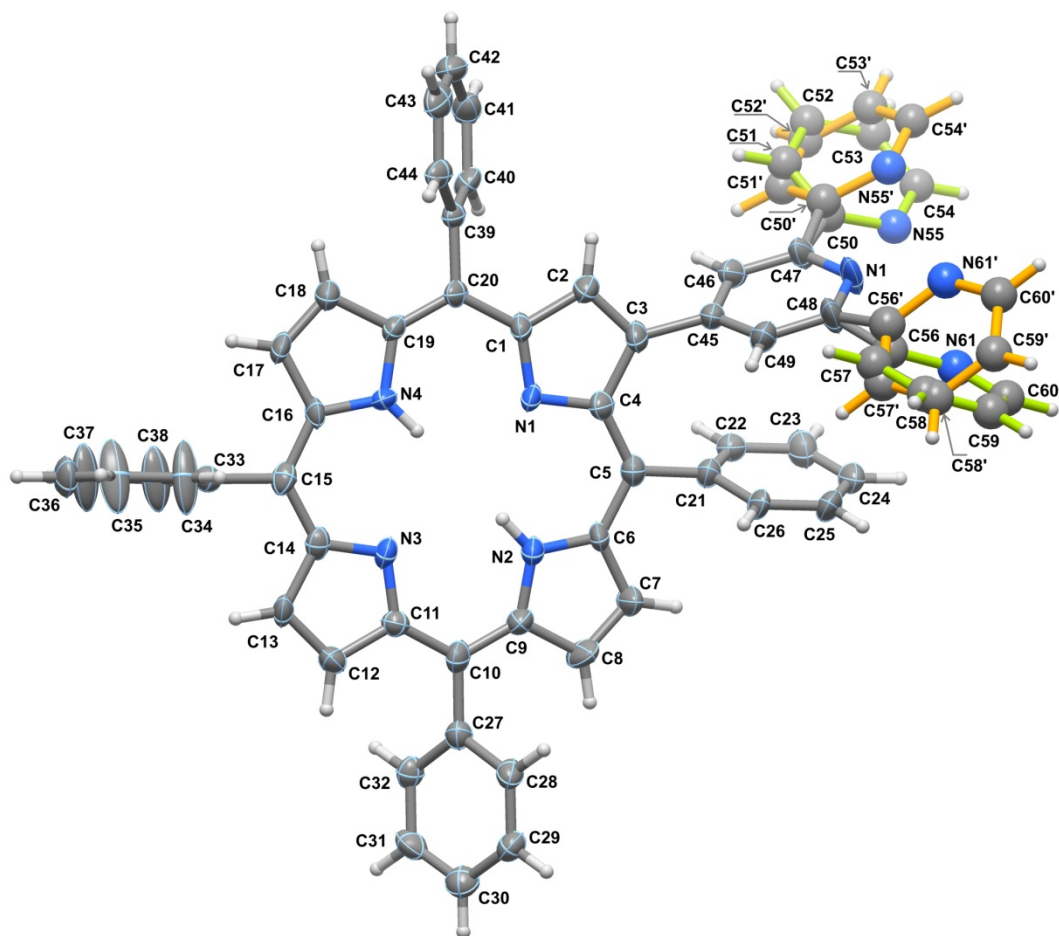


Figure S44. Schematic representation of the molecular unit composing the asymmetric unit of compound 3e. Non-hydrogen atoms belonging to the non-disordered portions of the molecule are represented as thermal ellipsoids drawn at the 50% probability level, while those composing the two peripheral and disordered pyridine moieties are represented in ball-and-stick. Hydrogen atoms are depicted as small spheres with arbitrary radius. The two locations of each disordered pyridine moiety (belonging to the substituent terpyridine) are represented with bonds having different colour (50% rate of occupancy for each location). The atomic labeling is provided for all non-hydrogen atoms.

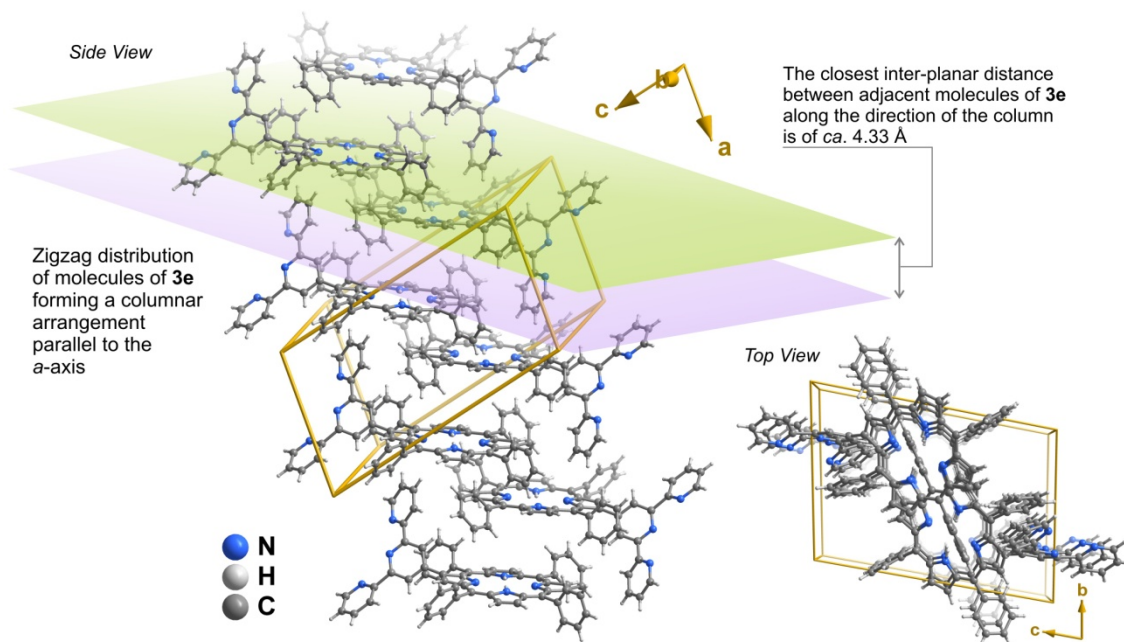


Figure S45. Close packing of adjacent molecular units of compound **3e** leading to the formation of a supramolecular column parallel to the *a*-axis of the unit cell. The distribution of molecular units is mostly driven by the need to effectively fill the available space because the closest inter-planar distance of ca. 4.33 Å.

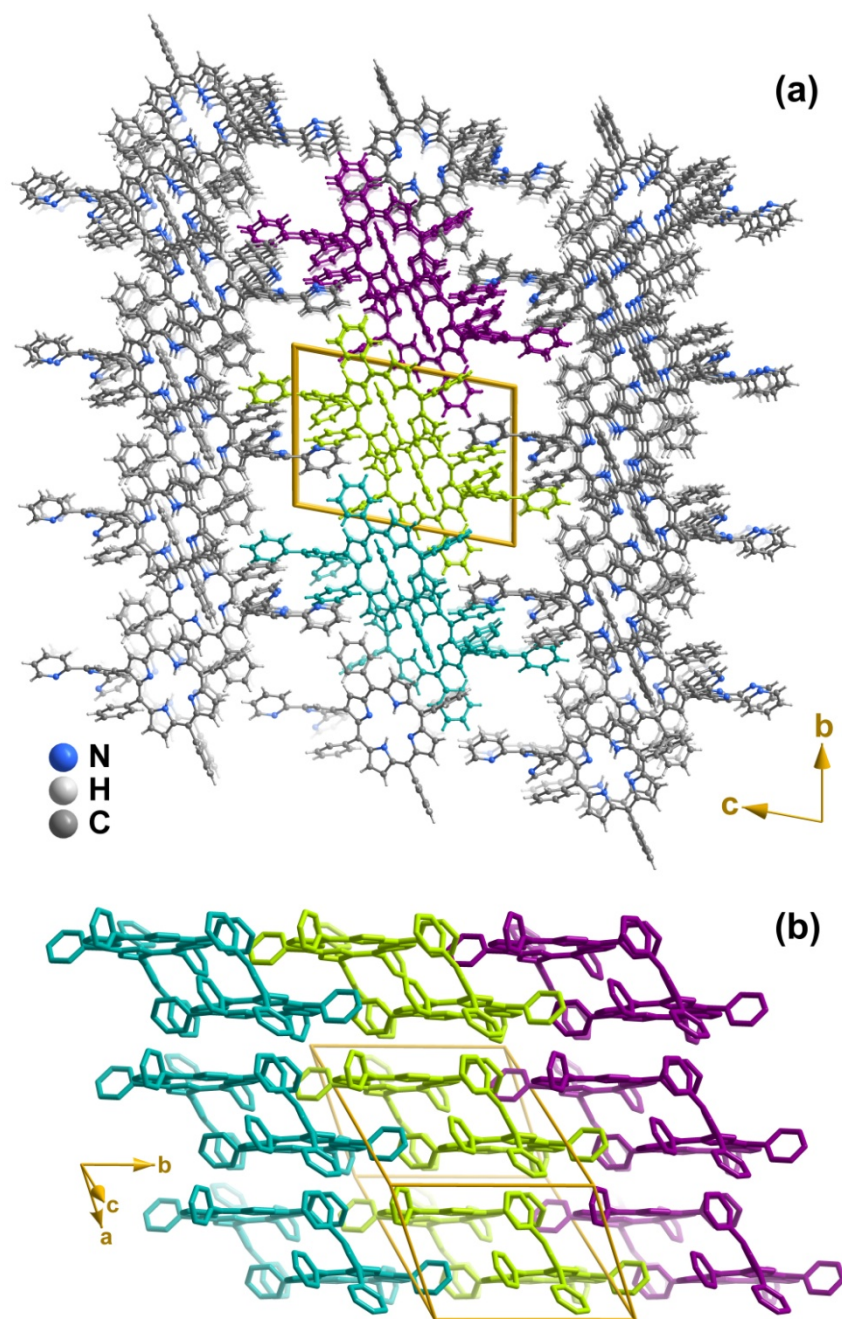


Figure S46. (a) Crystal packing of compound **3e** viewed in perspective along the [100] direction of the unit cell. For clarity, three of the supramolecular columnar arrangements of molecular units (as shown in Figure S5) are depicted at the center of the image in different colour. The packing of adjacent columns promotes the formation of voids which account for *ca.* 299 Å³ of the unit cell volume. (b) Side view of the three central supramolecular columns, emphasising that the crystal packing is essentially mediated by the need to effectively fill the available space. Hydrogen atoms have been omitted in this last representation for clarity purposes.

References

1. Armarego, W. L. F.; Perrin, D. D. *Purification of Laboratory Chemicals*, 4th Edt.; Butterworth-Heinemann: Oxford, 1996.
2. Moura, N. M. M.; Faustino, A. F.; Neves, M. G. M. P. S.; Costa, A. D.; Cavaleiro, J. A. S. *J. Porphyrins Phthalocyanines* 2011, **15**, 652-658.
3. T. Kottke and D. Stalke, *J. Appl. Crystallogr.*, 1993, **26**, 615-619.
4. APEX2, *Data Collection Software Version 2.1-RC13*, Bruker AXS, Delft, The Netherlands, 2006.
5. Cryopad, *Remote monitoring and control, Version 1.451*, Oxford Cryosystems, Oxford, United Kingdom, 2006.
6. SAINT+, *Data Integration Engine v. 7.23a* ©, 1997-2005, **Bruker AXS, Madison, Wisconsin, USA**.
7. G. M. Sheldrick, *SADABS v.2.01*, Bruker/Siemens Area Detector Absorption Correction Program, 1998, **Bruker AXS, Madison, Wisconsin, USA**.
8. G. M. Sheldrick, *SHELXS-97*, *Program for Crystal Structure Solution*, University of Göttingen, 1997.
9. G. M. Sheldrick, *Acta Cryst. A*, 2008, **64**, 112-122.
10. G. M. Sheldrick, *SHELXL-97*, *Program for Crystal Structure Refinement*, University of Göttingen, 1997.
11. A. L. Spek, *Acta Cryst. A*, 1990, **46**, C34.
12. A. L. Spek, *J. Appl. Crystallogr.*, 2003, **36**, 7-13.
13. P. van der Sluis and A. L. Spek, *Acta Cryst. A*, 1990, **46**, 194-201.